107

SATELLITE & MESOMETEOROLOGY
RESEARCH PROJECT

Department of the Geophysical Sciences
The University of Chicago

ANALISIS TROPICAL EN MESOESCALA SOBRE LATINO AMERICA

de

T. Theodore Fujita
Profesor de Meteorologia
Universidad de Chicago

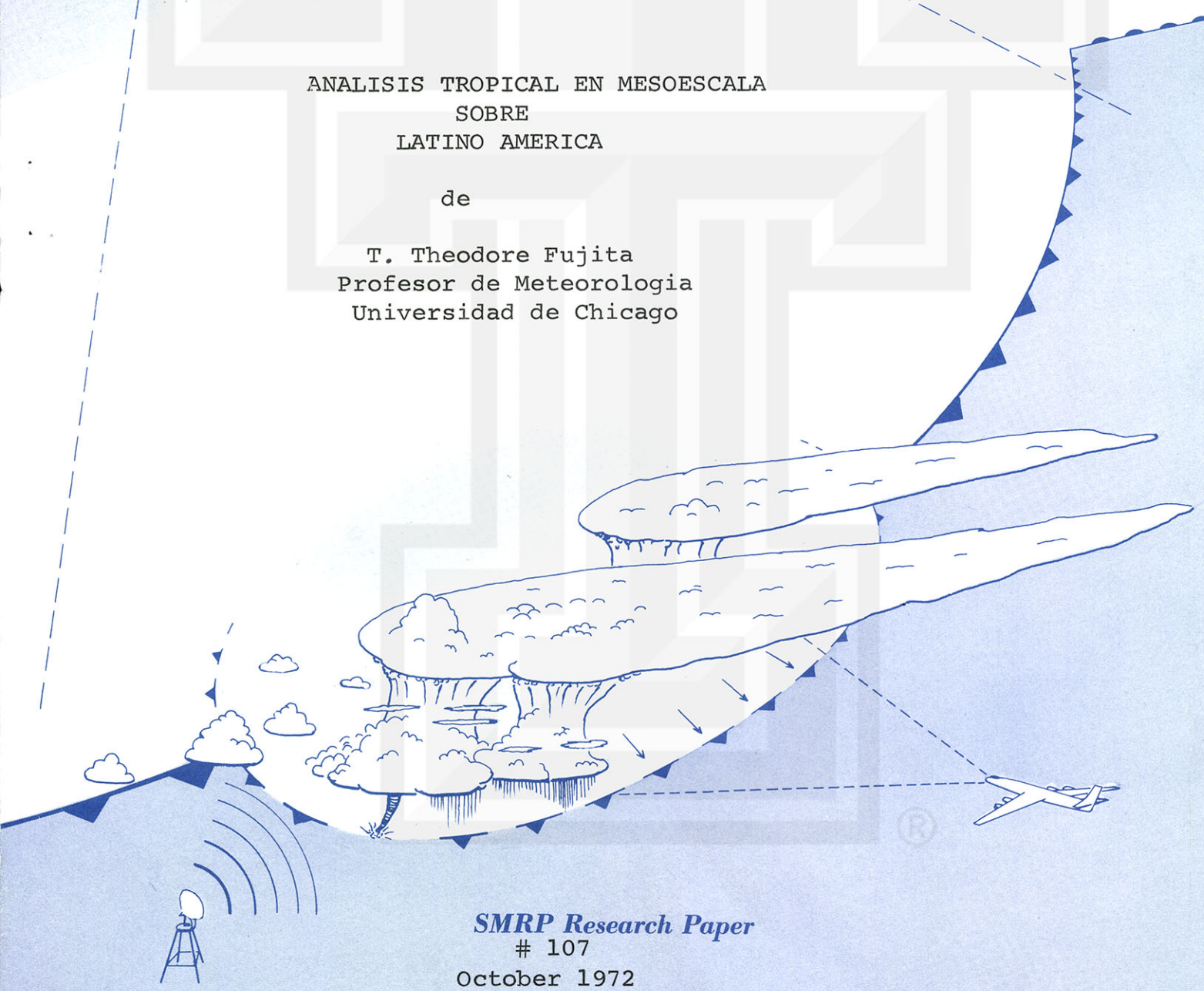

SMRP Research Paper
107
October 1972

MESOMETEOROLOGY PROJECT --- RESEARCH PAPERS

1.* Report on the Chicago Tornado of March 4, 1961 - Rodger A. Brown and Tetsuya Fujita

2.* Index to the NSSP Surface Network - Tetsuya Fujita

3.* Outline of a Technique for Precise Rectif.cation of Satellite Cloud Photographs - Tetsuya Fujita

4.* Horizontal Structure of Mountain Winds - Henry A. Brown

5.* An Investigation of Developmental Processes of the Wake Depression Through Excess Pressure Analysis of Nocturnal Showers - Joseph L. Goldman

6.* Precipitation in the 1960 Flagstaff Mesometeorological Network - Kenneth A. Styber

7.** On a Method of Single- and Dual-Image Photogrammetry of Panoramic Aerial Photographs - Tetsuya Fujita

8. A Review of Researches on Analytical Mesometeorology - Tetsuya Fujita

9.* Meteorological Interpretations of Convective Nephsystems Appearing in TIROS Cloud Photographs - Tetsuya Fujita, Toshimitsu Ushijima, William A. Hass, and George T. Dellert, Jr.

10.* Study of the Development of Prefrontal Squall-Systems Using NSSP Network Data - Joseph L. Goldman

11. Analysis of Selected Aircraft Data from NSSP Operation, 1962 - Tetsuya Fujita

12. Study of a Long Condensation Trail Photographed by TIROS I - Toshimitsu Ushijima

13. A Technique for Precise Analysis of Satellite Data; Volume I - Photogrammetry (Published as MSL Report No. 14) - Tetsuya Fujita

14. Investigation of a Summer Jet Stream Using TIROS and Aerological Data - Kozo Ninomiya

15. Outline of a Theory and Examples for Precise Analysis of Satellite Radiation Data - Tetsuya Fujita

16. Preliminary Result of Analysis of the Cumulonimbus Cloud of April 21, 1961 - Tetsuya Fujita and James Arnold

17. A Technique for Precise Analysis of Satellite Photographs - Tetsuya Fujita

18.* Evaluation of Limb Darkening from TIROS III Radiation Data - S.H.H. Larsen, Tetsuya Fujita, and W.L. Fletcher

19. Synoptic Interpretation of TIROS III Measurements of Infrared Radiation - Finn Pedersen and Tetsuya Fujita

20.* TIROS III Measurements of Terrestrial Radiation and Reflected and Scattered Solar Radiation - S.H.H. Larsen, Tetsuya Fujita, and W.L. Fletcher

21. On the Low-level Structure of a Squall Line - Henry A. Brown

22.* Thunderstorms and the Low-level Jet - William D. Bonner

23.* The Mesoanalysis of an Organized Convective System - Henry A. Brown

24. Preliminary Radar and Photogrammetric Study of the Illinois Tornadoes of April 17 and 22, 1963 - Joseph L. Goldman and Tetsuya Fujita

25. Use of TIROS Pictures for Studies of the Internal Structure of Tropical Storms - Tetsuya Fujita with Rectified Pictures from TIROS I Orbit 125, R/O 128 - Toshimitsu Ushijima

26. An Experiment in the Determination of Geostrophic and Isallobaric Winds from NSSP Pressure Data - William Bonner

27. Proposed Mechanism of Hook Echo Formation - Tetsuya Fujita with a Preliminary Mesosynoptic Analysis of Tornado Cyclone Case of May 26, 1963 - Tetsuya Fujita and Robbi Stuhmer

28. The Decaying Stage of Hurricane Anna of July 1961 as Portrayed by TIROS Cloud Photographs and Infrared Radiation from the Top of the Storm - Tetsuya Fujita and James Arnold

29. A Technique for Precise Analysis of Satellite Data, Volume II - Radiation Analysis, Section 6. Fixed-Position Scanning - Tetsuya Fujita

30. Evaluation of Errors in the Graphical Rectification of Satellite Photographs - Tetsuya Fujita

31. Tables of Scan Nadir and Horizontal Angles - William D. Bonner

32. A Simplified Grid Technique for Determining Scan Lines Generated by the TIROS Scanning Radiometer - James E. Arnold

33. A Study of Cumulus Clouds over the Flagstaff Research Network with the Use of U-2 Photographs - Dorothy L. Bradbury and Tetsuya Fujita

34. The Scanning Printer and Its Application to Detailed Analysis of Satellite Radiation Data - Tetsuya Fujita

35. Synoptic Study of Cold Air Outbreak over the Mediterranean using Satellite Photographs and Radiation Data - Aasmund Rabbe and Tetsuya Fujita

36. Accurate Calibration of Doppler Winds for their use in the Computation of Mesoscale Wind Fields - Tetsuya Fujita

37. Proposed Operation of Intrumented Aircraft for Research on Moisture Fronts and Wake Depressions - Tetsuya Fujita and Dorothy L. Bradbury

38. Statistical and Kinematical Properties of the Low-level Jet Stream - William D. Bonner

39. The Illinois Tornadoes of 17 and 22 April 1963 - Joseph L. Goldman

40. Resolution of the Nimbus High Resolution Infrared Radiometer - Tetsuya Fujita and William R. Bandeen

41. On the Determination of the Exchange Coefficients in Convective Clouds - Rodger A. Brown

* Out of Print
** To be published

(Continued on back cover)

1. INTRODUCTION

The Earth's equator is no longer the magic circle separating the northern and southern hemispheres. The atmosphere moves freely across the equator as do the clouds seen in satellite pictures.

Cross-equatorial motion of clouds over the ocean is much simpler than over the continent where local topography and thermal effects give rise to the development and dissipation of traveling clouds.

Cloud-motion vectors superimposed upon the NOAA mosaic of September 17, 1967[1] reveal that the low clouds cross the equator to move into the zone of intertropical convergence. The ITCZ is characterized by both convergence and cyclonic vorticity which is not uniform along the zone. There are local centers which are identified as "cloud clusters". A cloud cluster, including a large number of much smaller convective elements, is a large cloud mass topped by extensive cirrus clouds.

ITCZ is not well defined over the continent where the competition of convective clouds is so large that each will be given a chance to grow into a "pop corn" thunderstorm.

Presented in this paper is a result of day-by-day analyses of equatorial Latin America for an 11-day period in September, 1967.

---

[1] For further detail, refer to Fujita, Watanabe, and Izawa (1969), Formation and Structure of Equatorial Anticyclones caused by Large-scale Cross-equatorial Flows Determined by ATS-I Photographs, J. Appl. Meteor., Vol. 8, pp. 649-667.

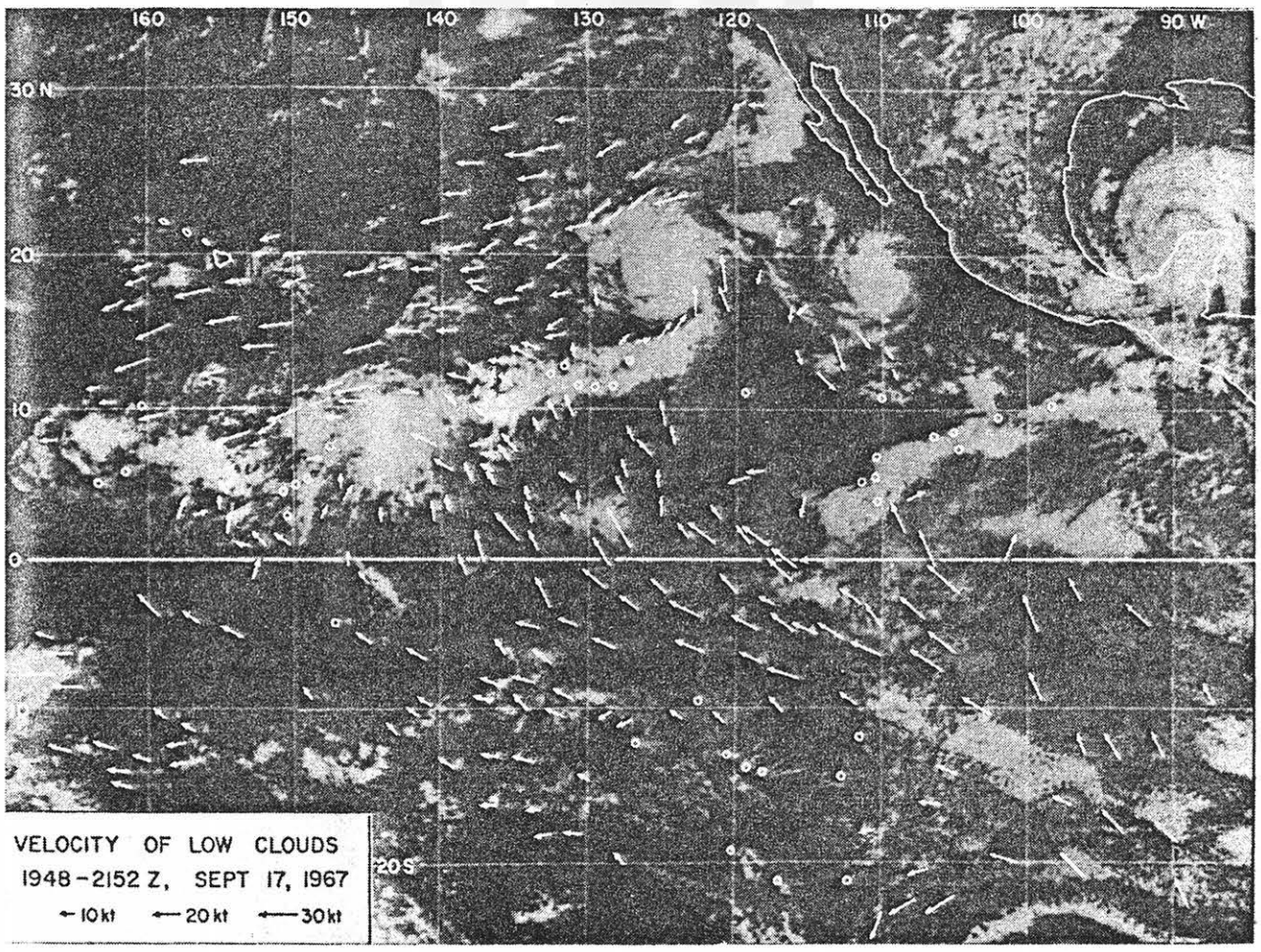

2. MEAN CLOUD COVER IN SEPTEMBER 1967-70

The mean cloud-cover picture presented in this chapter was produced jointly by NOAA and U.S. Air Force.[2] The picture was generated by computer processing of the original photographic signal of AVCS pictures taken at 2 PM local time.

White areas in the picture indicate the high values of mean brightness, contributed by clouds and their background. Note that Salar de Uyuni is white and Lago Titicaca is black.

Extensive stratus clouds are seen over Humboldt Current (Peru current) which is a cold upwelling current. A cloud band extending east-west just north of Islas Galapagos is likely to be stratus, but the one to the south of Panama consists of deep convective clouds.

There is a long line of cloudiness along the southeast coast of Brazil. Both off-shore winds and the up-slope motion are responsible to the formation of this cloud band.

The mid Atlantic ITCZ cloud band does not extend all the way to the Guiana coast. Instead, the band extends west-northwest, parallel to the coast.

---

[2] Global Atlas of Relative Cloud Cover, 1967-70, based on Photographic Signal from Meteorological Satellites. U.S. Department of Commerce and U.S. Air Force. September 1971.

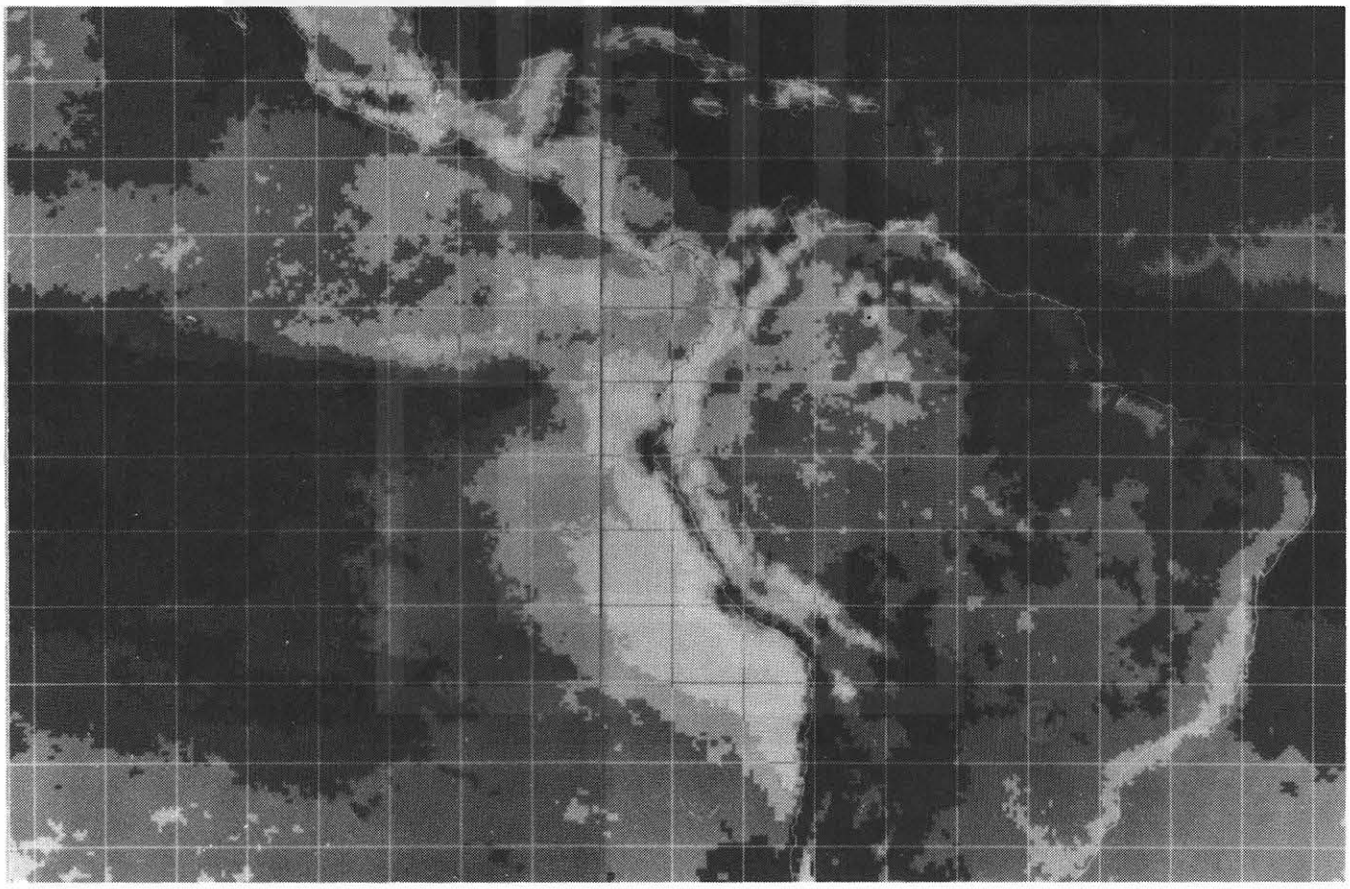

3. MEAN CLOUD COVER, SEPTEMBER 8-18, 1967

The mean cloud-cover picture on this page was produced by superimposing the 11 daily pictures shown in Chapter 5.

The mean position of the ITCZ for this period is indicated by a heavy line. The line almost coincides with the axis of extensive cloudiness over the Pacific, far away from land areas.

Off the coast of Central America, however, there are dark areas on or just to the northeast of the ITCZ. These areas are located in the rain shadow of the east-northeasterlies which unload heavy precipitation over Guatemala and Costa Rica.

The ITCZ in the Caribbean off the coast of Venezuela runs through a band of dark area. The southeasterly flow descending into the Caribbean after moving over the coastal range of Venezuela is too dry to form a band of ITCZ cloudiness. The east end of the ITCZ coincides with the axis of the cloud band extending to Africa.

An extensive area of clouds, extending from Barbados to the tip of Yucatan peninsula, corresponds to the track of hurricane Beulah and easterly waves forming in the Atlantic ITCZ to move away toward the west-northwest.

Directions of the prevailing flow, entering the Amazon basin and turning south toward southern Brazil, can be seen as cloud streaks which tend to extend in the direction of low-level flow.

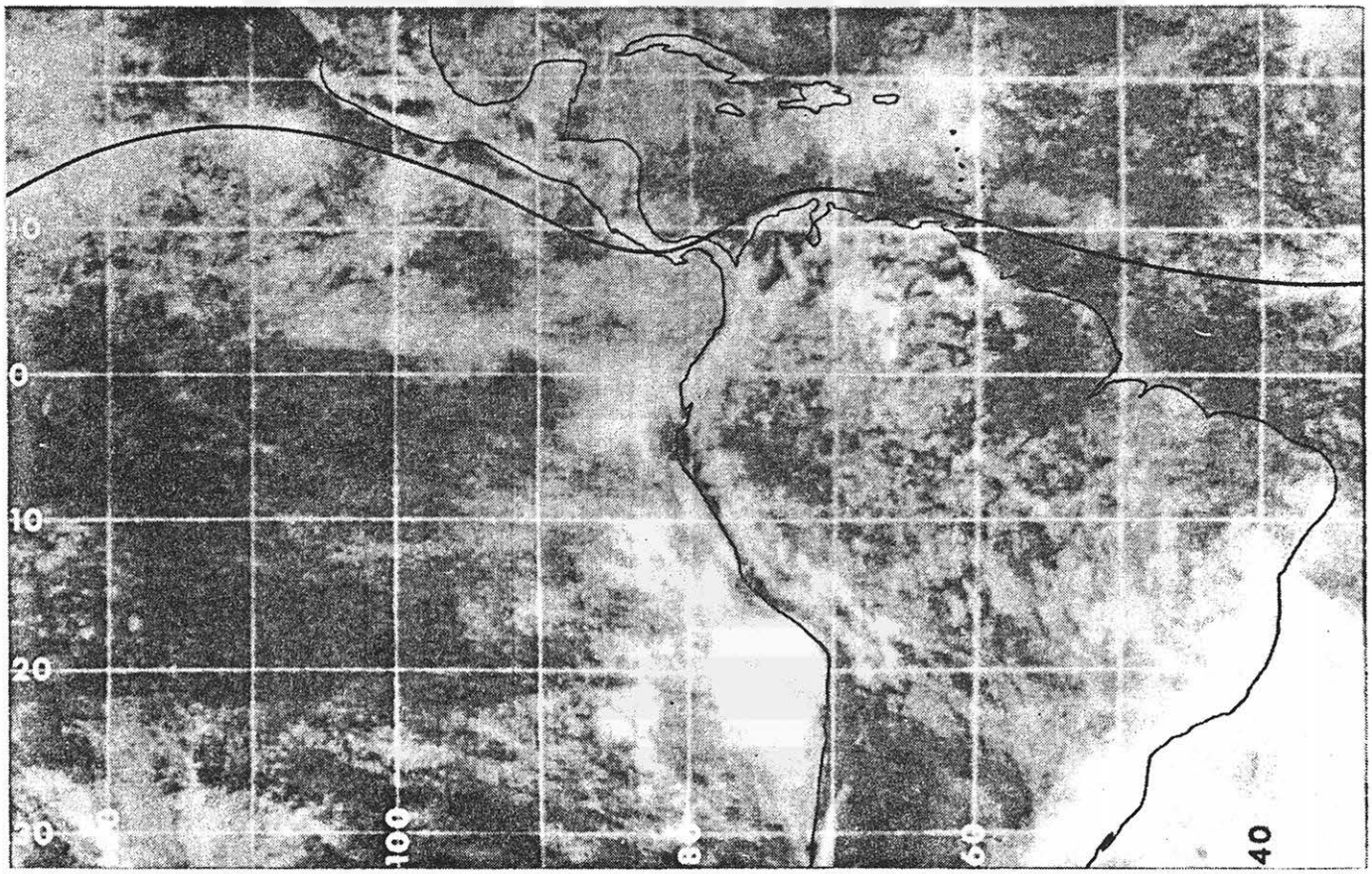

4. ITCZ, FRONTS AND OCEAN CURRENT

This figure includes composite positions of the ITCZ copied from the daily synoptic analyses in Chapter 5. Zonal variation of the ITCZ was very large over the Pacific, south of Baja California, where cloud clusters formed and moved out toward a north-northwesterly direction. The variation was also significant over the northern part of South America due, mainly, to the changes in the stream lines originating in both the northern and southern hemisphere.

ITCZ is defined in the Glossary of Meteorology, American Meteorological Society, 1959, as being the axis which divides the broad current of trade wind in the northern and southern hemispheres. The word "ITCZ" is often used to represent a zone of convergence which is wider than the intertropical front.

Cold fronts in the southern hemisphere are shown with double lines. They form just behind the southern Andes and move rapidly into the vast plain of South America. Regions of the Andes Mountains above 2,000 m are stippled.

Included also in the figure are the mean ocean currents. Dashed arrows represent warm current and solid arrows, cold current. Humboldt current flows northwest toward the equator, where it changes into the Equatorial current.

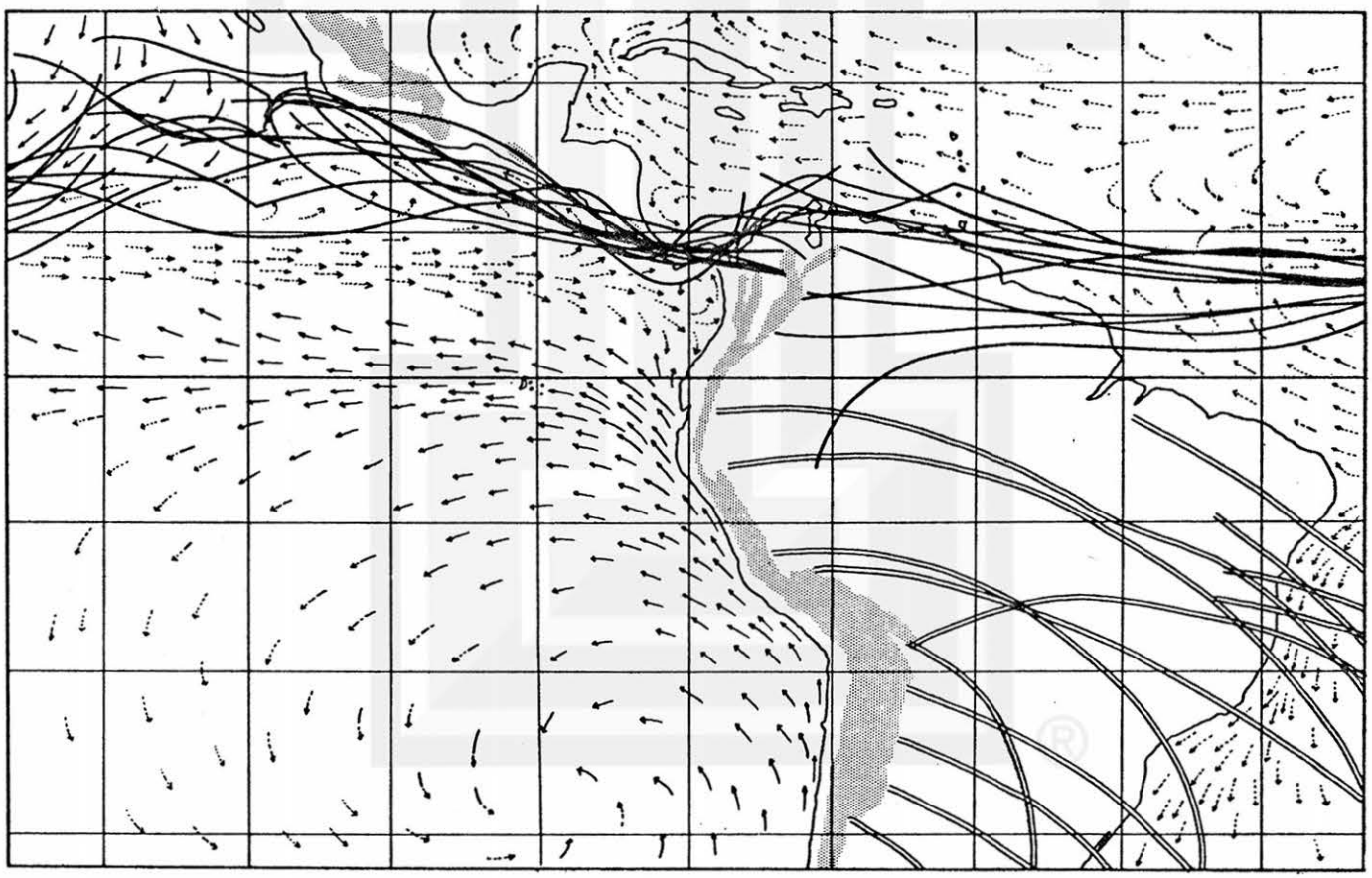

5. DAILY ANALYSES, SEPTEMBER 8-18, 1967

The following tropical analyses, covering an 11-day period, revealed synoptic aspects of pressure and flow patterns along with mesoscale nephsystems in NOAA mosaic pictures.

Isobars are drawn for every 2 mb. Stream lines are over-printed in red. The crossing angle of the air, as it travels from southern to northern hemisphere, varies from about 150 to 30 reaching 90 shortly after the equator crossing.

SEPTEMBER 8, 1967

ITCZ is not too distinct on this day. A recognizable but insignificant ITCZ, near the east edge of the map, disappears toward the west. The boundary between northern and southern trade wind is, nevertheless, shown in a dashed line.

There are three lows along the ITCZ. The first one is over Panama, the second to the south of Mexico, and the third on 122W longitude. Hurricane Beulah is seen over the eastern Caribbean.

A major cold front extends from Bolivia to southern Brazil. This front is accompanied by a wide band of cloudiness which ends sharply along the east slope of the Andes.

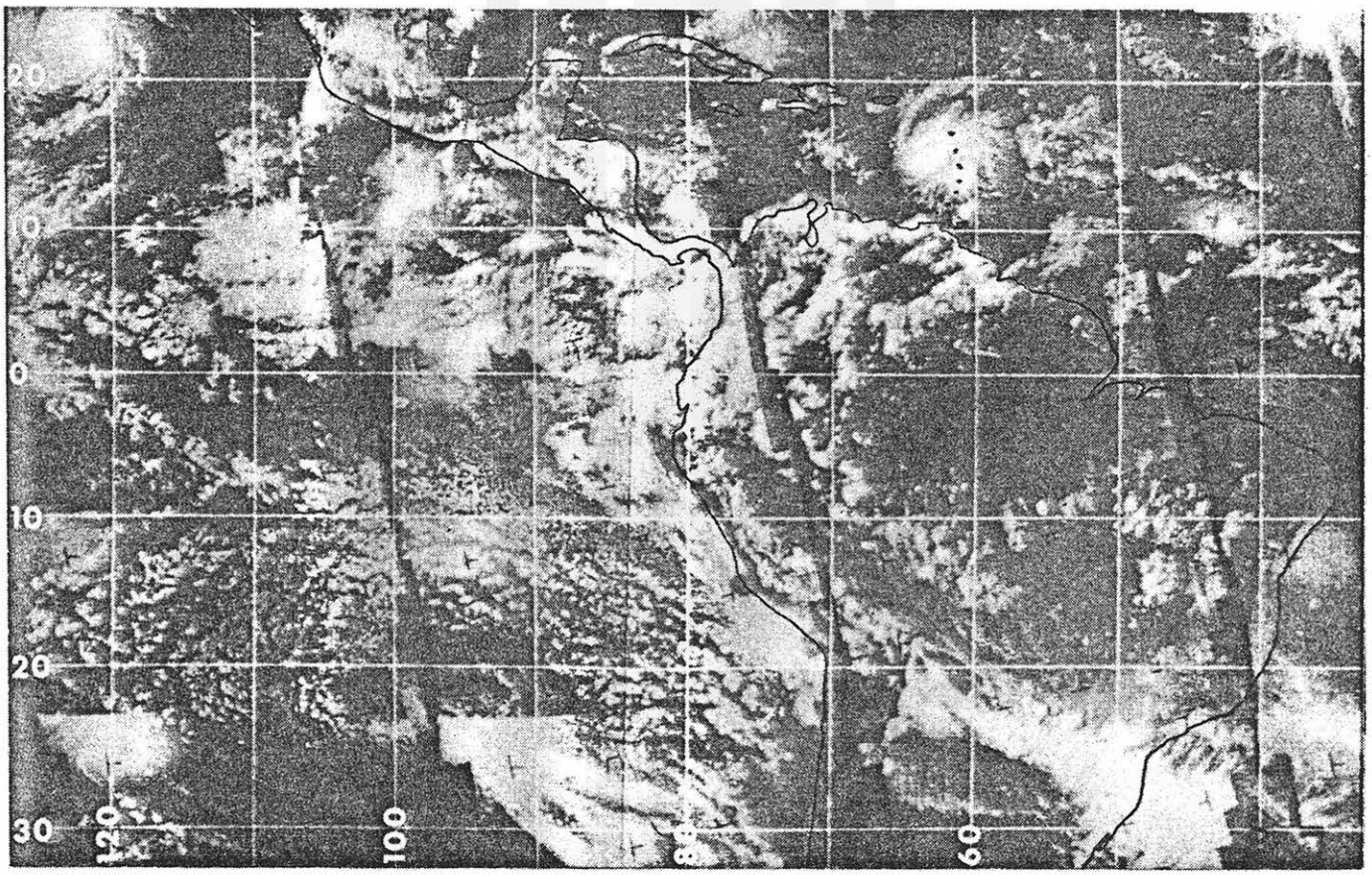

SEPTEMBER 8, 1967

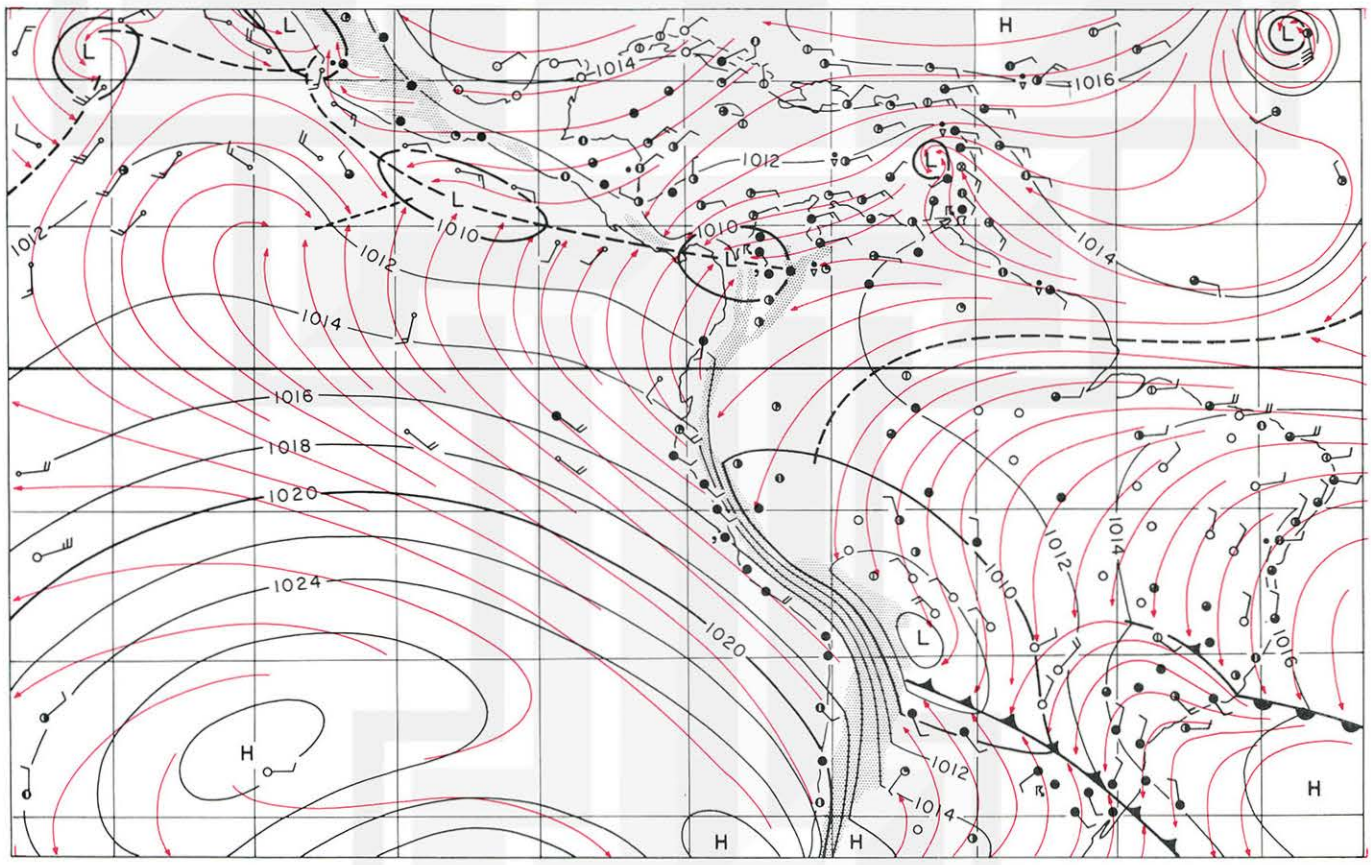

SEPTEMBER 9, 1967

There is no major change in the Pacific except a 2-mb rise in the central pressure of the South Pacific high. The ITCZ moved south to about 10 S, meanwhile a tropical storm at 120 W moved north out of the map area. Hurricane Beulah is moving west in the Caribbean south of Puerto Rico.

Southern hemisphere stream lines shifted north, pushing the ITCZ toward Lake Maracaibo. The entire Amazon basin is under the influence of easterlies and practically cloud free.

The cold front advanced rapidly, now extending from northern Bolivia to Rio de Janeiro. The cloud band along this front over the continent is quickly breaking up. It is hard to explain the existence of a large cloud mass just north of Brasilia where the center of a small anticyclone is located.

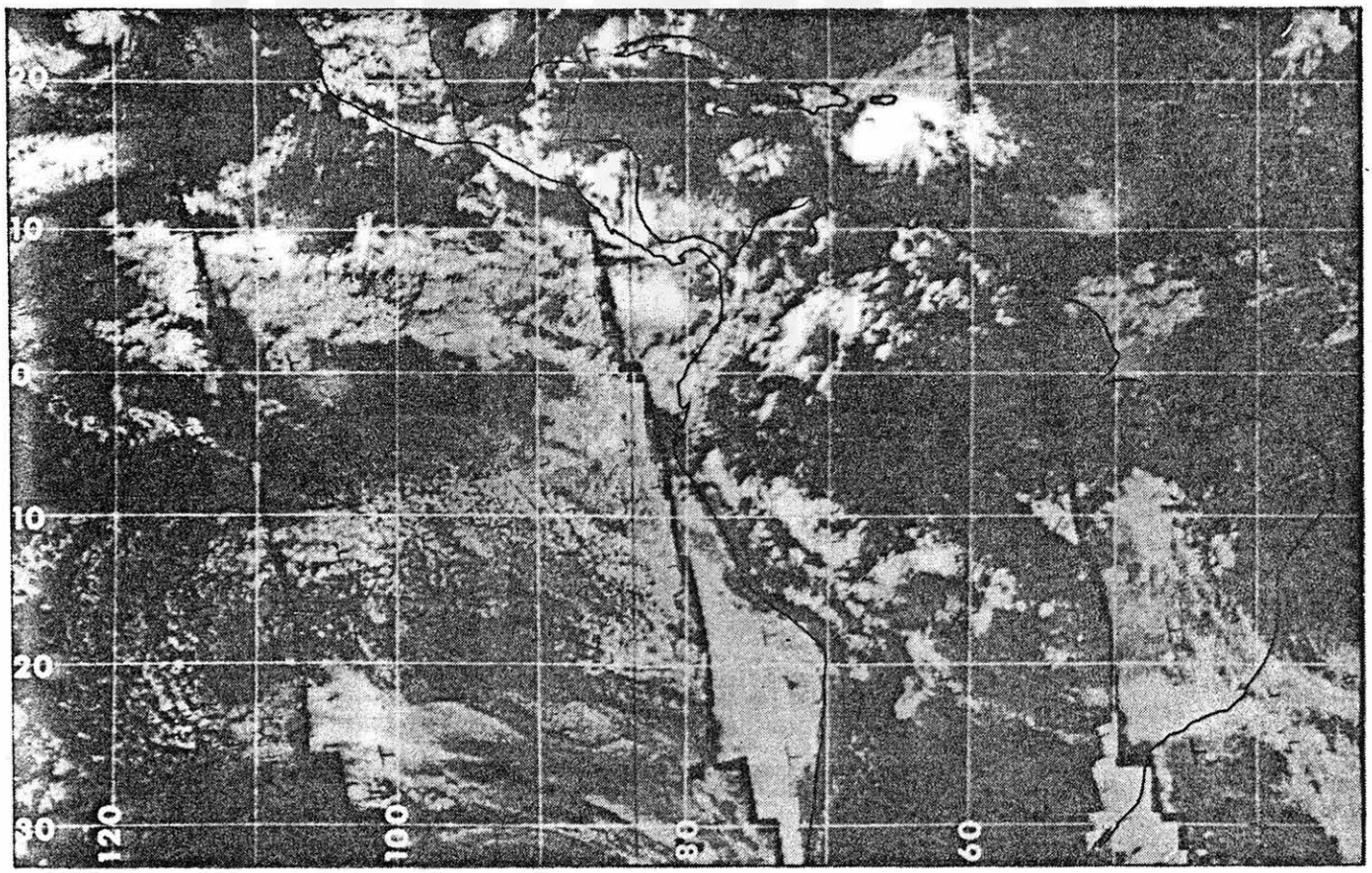

SEPTEMBER 9, 1967

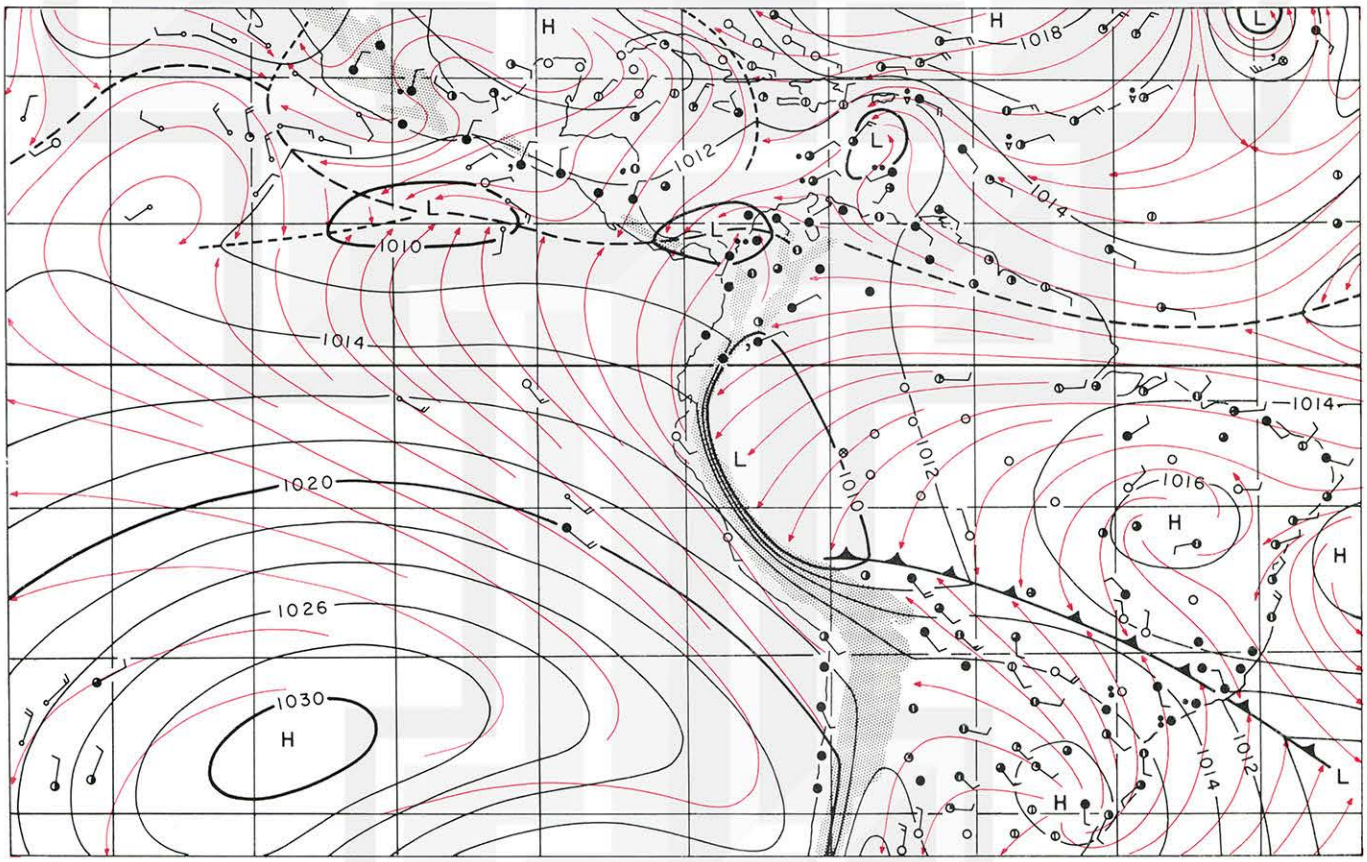

SEPTEMBER 10, 1967

The west end of the cold front which reached northern Bolivia on the 9th is now moving back southward while its air-mass contrast decreased considerably. The eastern portion has been pushing northeast steadily, being accompanied by a narrow band of cloudiness off the Brazilian coast.

The entire area of South America east of Andes Mountains is under the influence of easterlies from the South Atlantic. Land convection has increased since the previous day, but it is still insignificant. The southern hemisphere trade wind is probably very dry.

A short wave upper-air trough in the westerlies appears to be located at 90 W, according to the broad-scale curvature of cloud bands. Cold air advection to the north of the surface low at 40 W and warm air advection just to the east of the Andes created a 15 mb difference in the surface pressure across the Andes at 30 S.

There is no major change in ITCZ in the Atlantic or Pacific, while Hurricane Beulah just to the south of Santo Domingo is moving west.

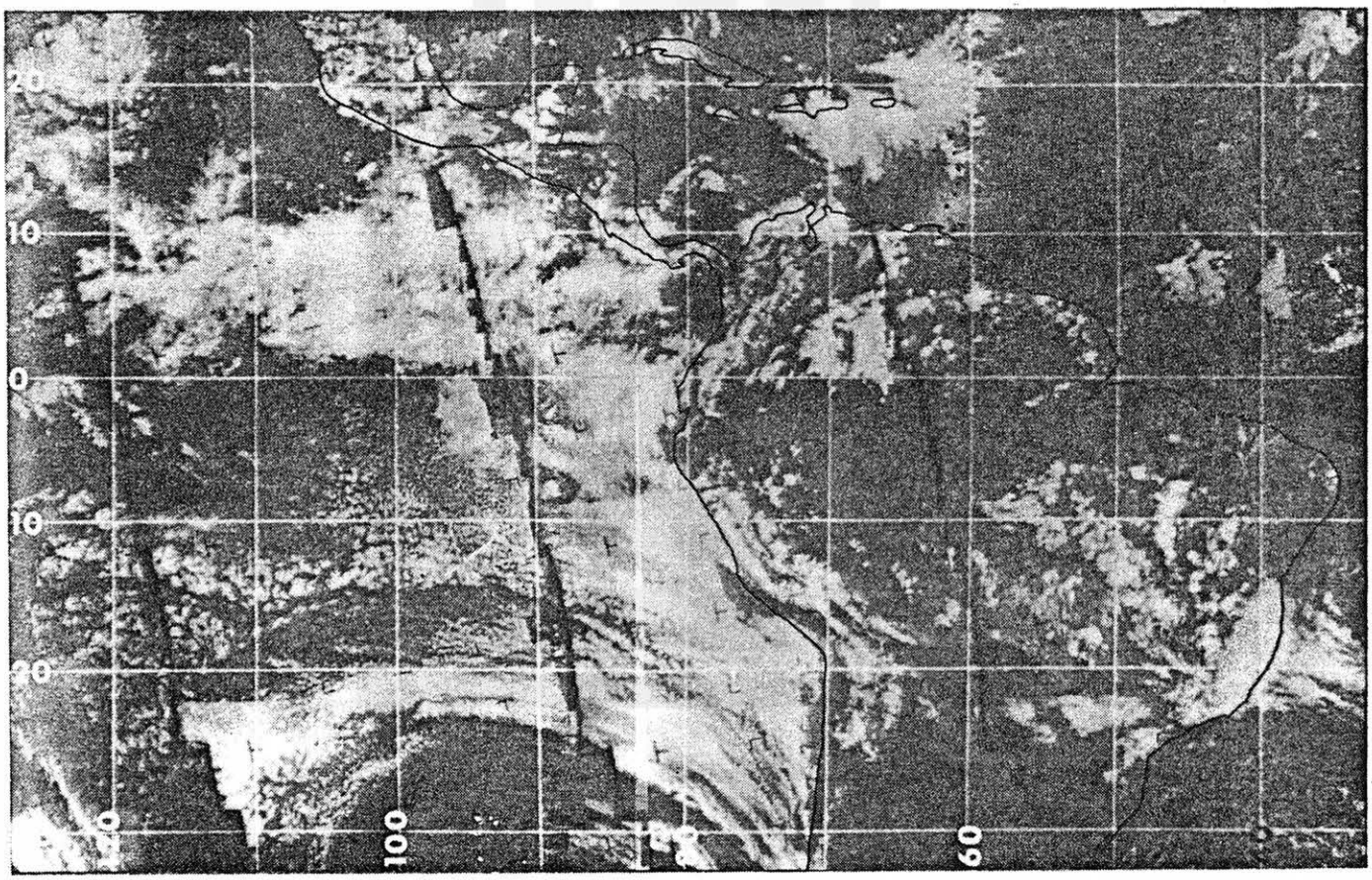

SEPTEMBER 10, 196

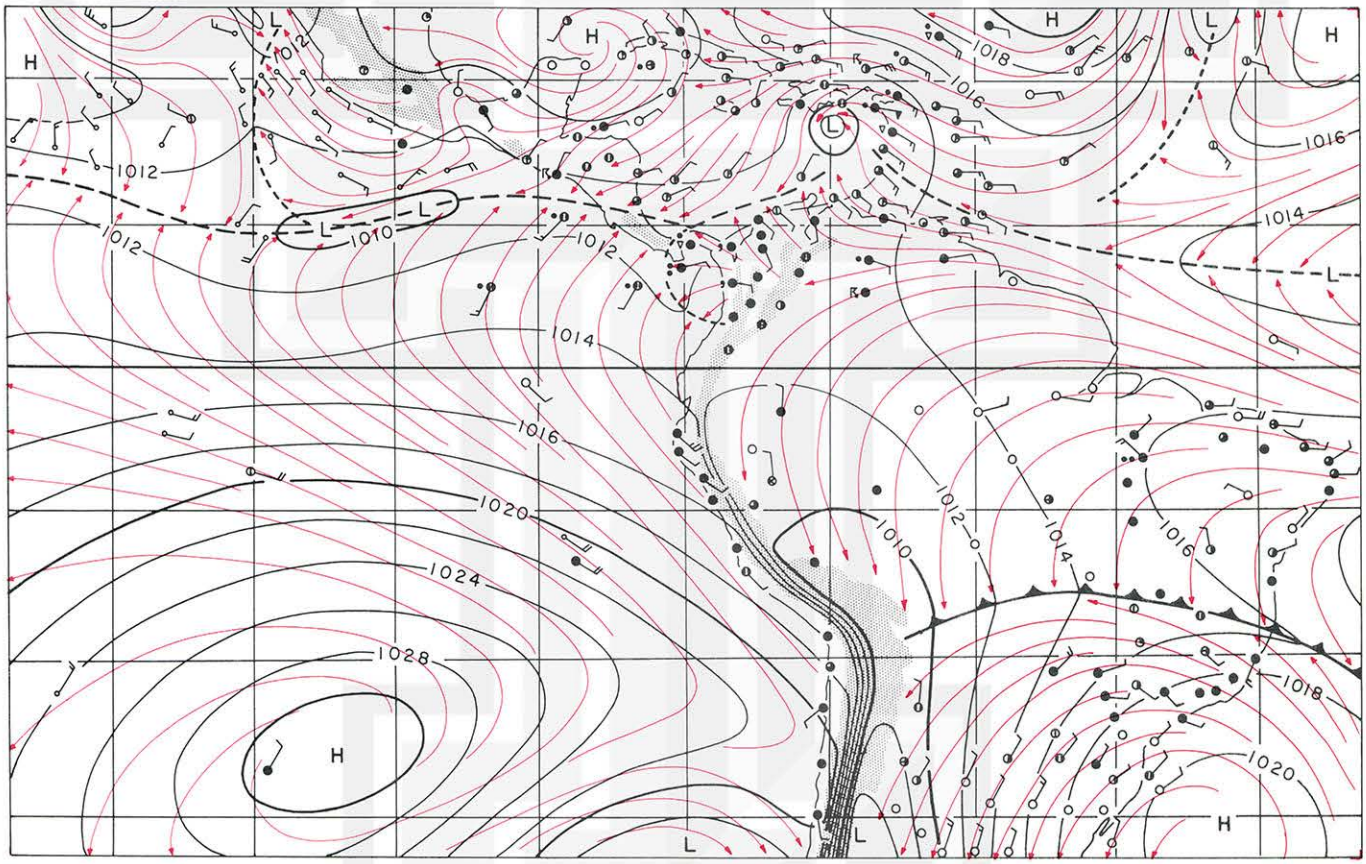

SEPTEMBER 11, 1967

Middle cloud band extending from northernmost Chile, Asuncion to Rio de Janeiro, suggests that a ridge in the westerlies is located just about 55W. This cloud band is seen on both sides of the Bolivian Andes, suggesting that the height would be about 500 mb.

A 25 mb difference in the surface pressure on both sides of the Andes at 30 S is rather spectacular. We do not expect to see such an orographic pressure gradient in other parts of the world. Andes Mountains act like a great, tall wall.

The ITCZ in the Pacific moved north due probably to the increased cross-equatorial flow. There are two lows between 100 and 110 W at the locations of growing cloud clusters.

Hurricane Beulah, over the central Caribbean, is accompanied by a huge cloud mass extending to the east. This cloud mass is seen within the cold air mass being fed into the storm.

It should be pointed out that the pictures from the orbit with 125 W ascending node are misplaced, due probably to an error in the subsatellite point.

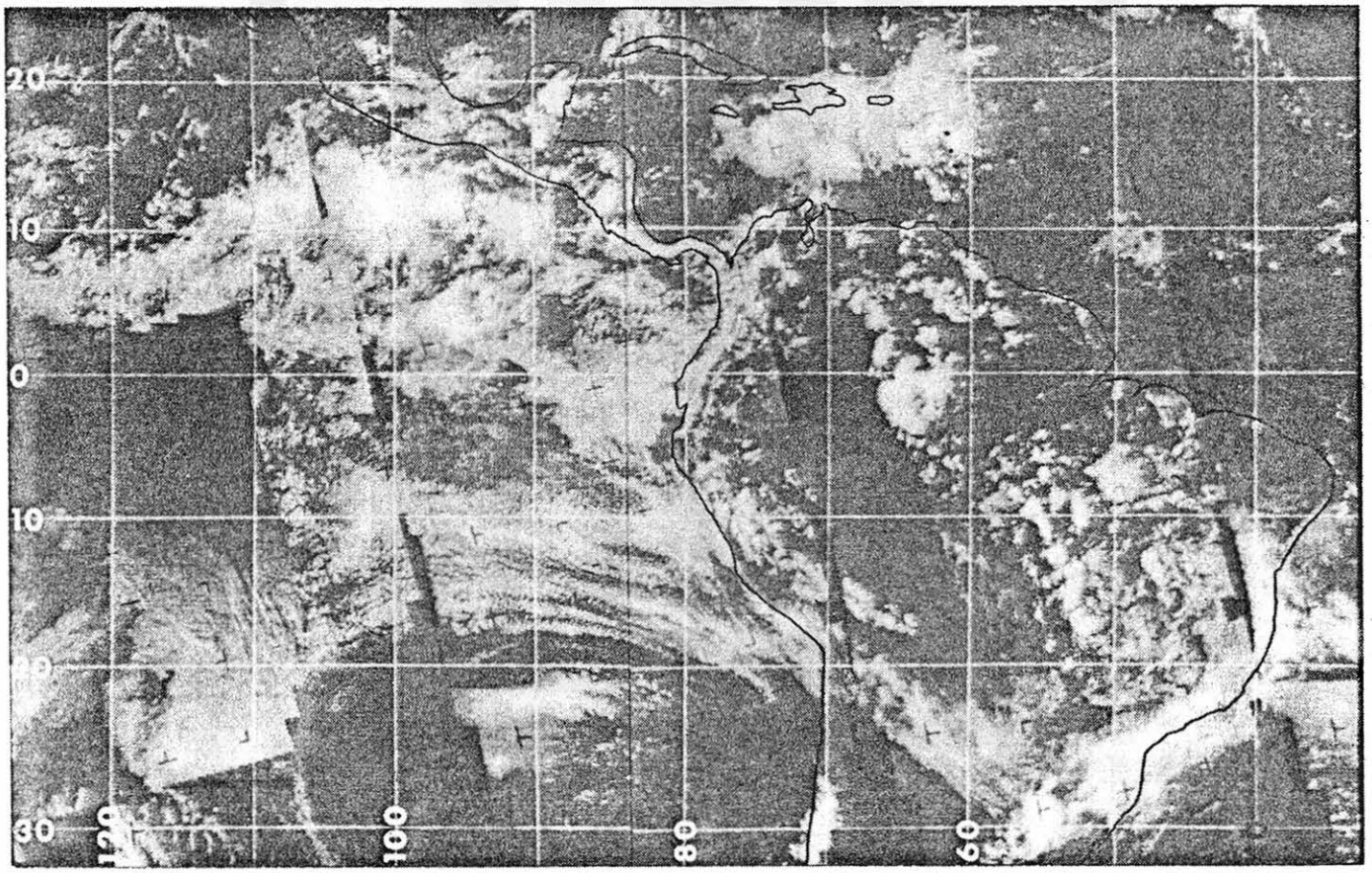

SEPTEMBER 11, 1967

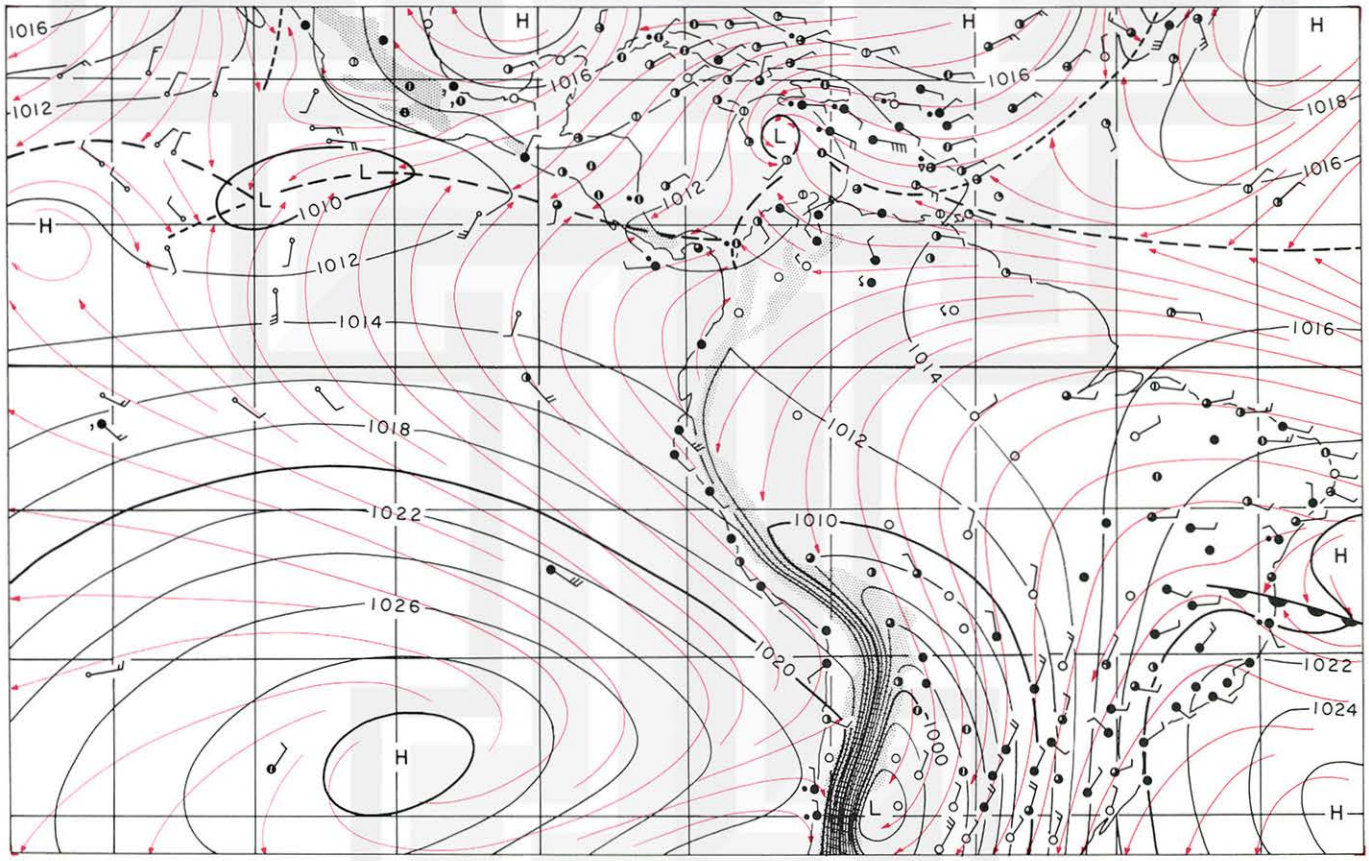

SEPTEMBER 12, 1967

The cold air advected north over Argentina increased the surface pressure by 20 mb in one day, thus reducing the surface pressure difference on both sides of the Andes to only a few mb. The cold front now extends from central Bolivia to Uruguay. The map time, 1200 GMT, and satellite picture time, 1400 Local Standard Time, are 6 hr apart. Thus, the cloud band moved ahead of the front due to this time difference.

Typical air-mass convection is seen over tropical South America east of the Andes. Note that streaks of convective clouds are parallel to the surface stream lines. Surface friction and little effects of Coriolis force result in a right-angle crossing between stream lines and isobars near the equator. The pressure gradient simply draws maritime easterly wind into the Amazon basin against surface friction while maintaining near 90 crossing angle.

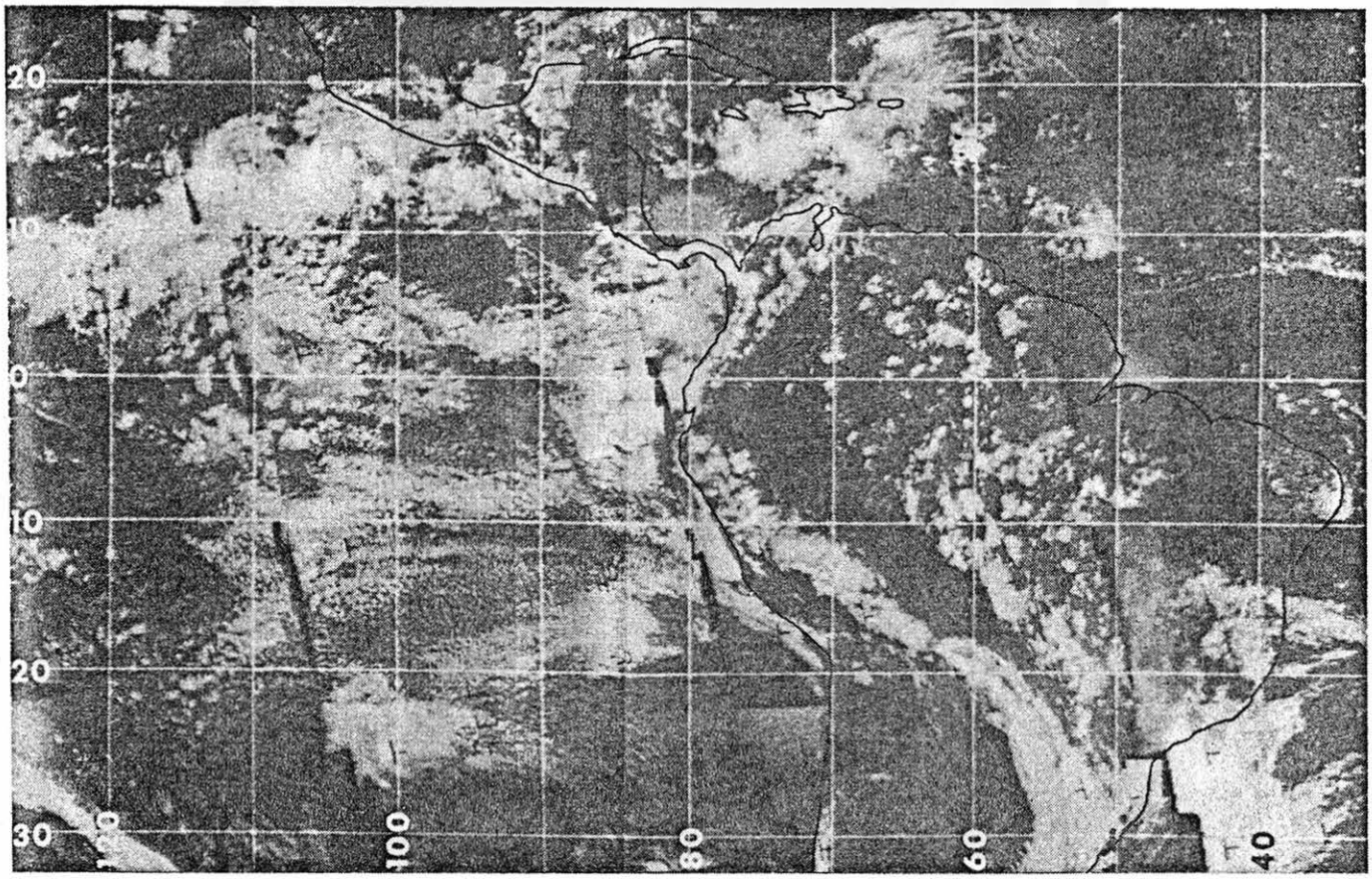

SEPTEMBER 12, 1967

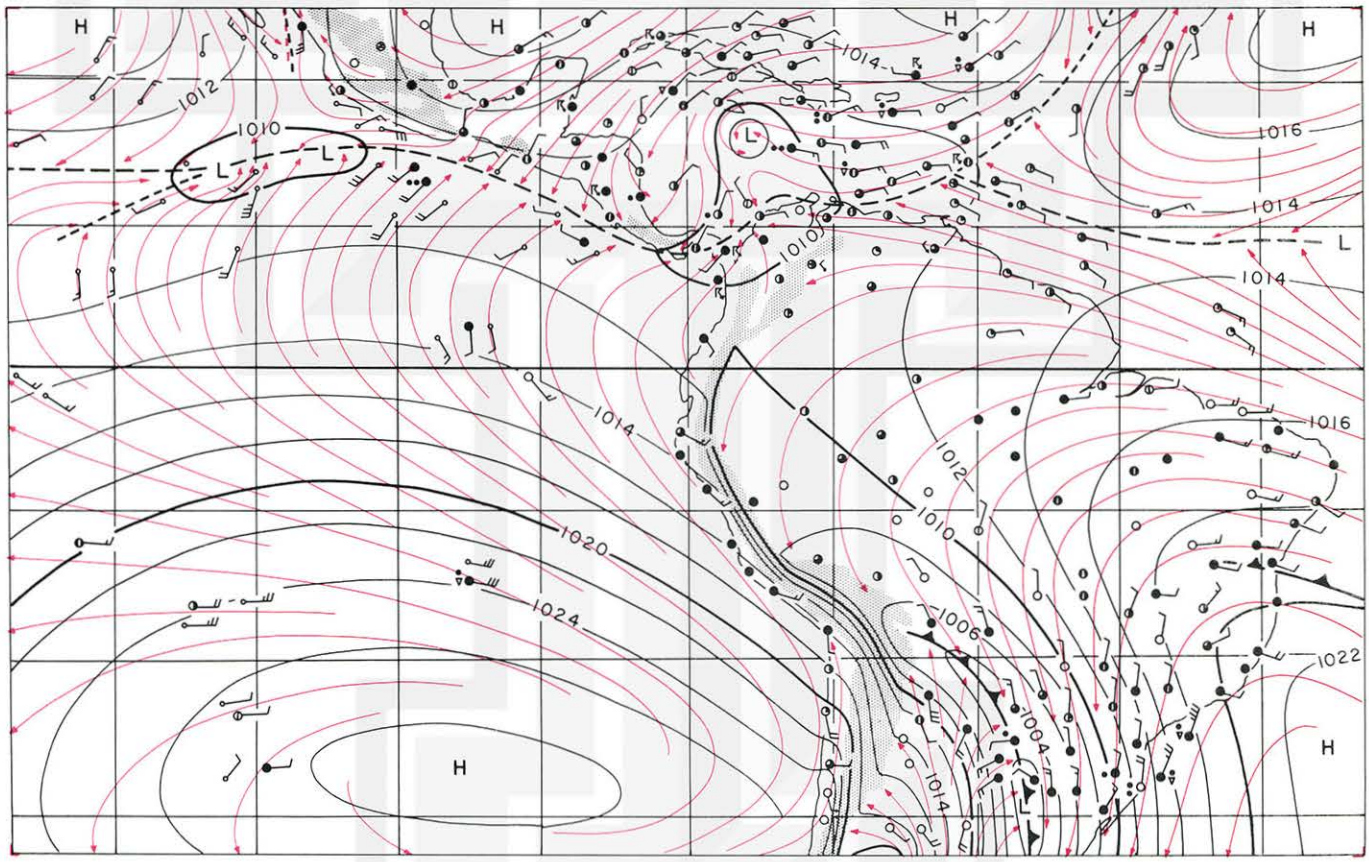

SEPTEMBER 13, 1967

A beautiful example of a southern hemisphere cold-air outflow is seen over central South America. The center of a traveling anticyclone with 1025 mb central pressure is seen over Asuncion, Paraguay. The pressure gradient across the Andes is now reversed.

The entire area of Brazil located ahead of the cold front is dominated by the easterlies. The frontal cloud band is extensive being characterized by the underlying band of convergence.

Two cloud clusters on the 106 W and 116 W longitudes begin showing a circulation structure. Meanwhile, hurricane Beulah is intensifying in the Caribbean south of Jamaica. Beulah is drawing, in part, a southwesterly flow of southern hemisphere origin. An insignificant ITCZ running between parallel stream lines extends from Beulah area to Trinidad Island on to the mid Atlantic cloud band along the 7 N latitude.

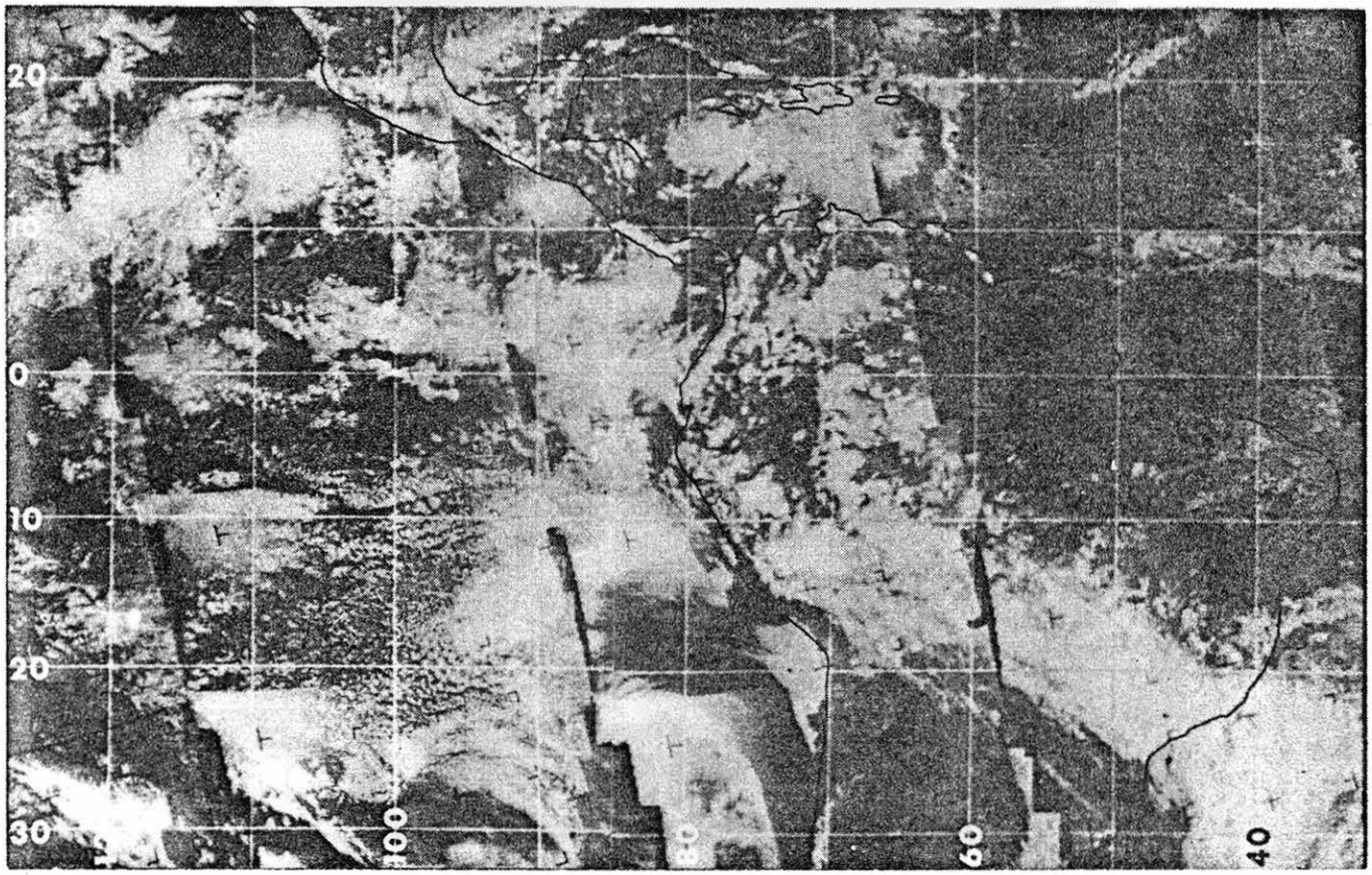

SEPTEMBER 13, 1967

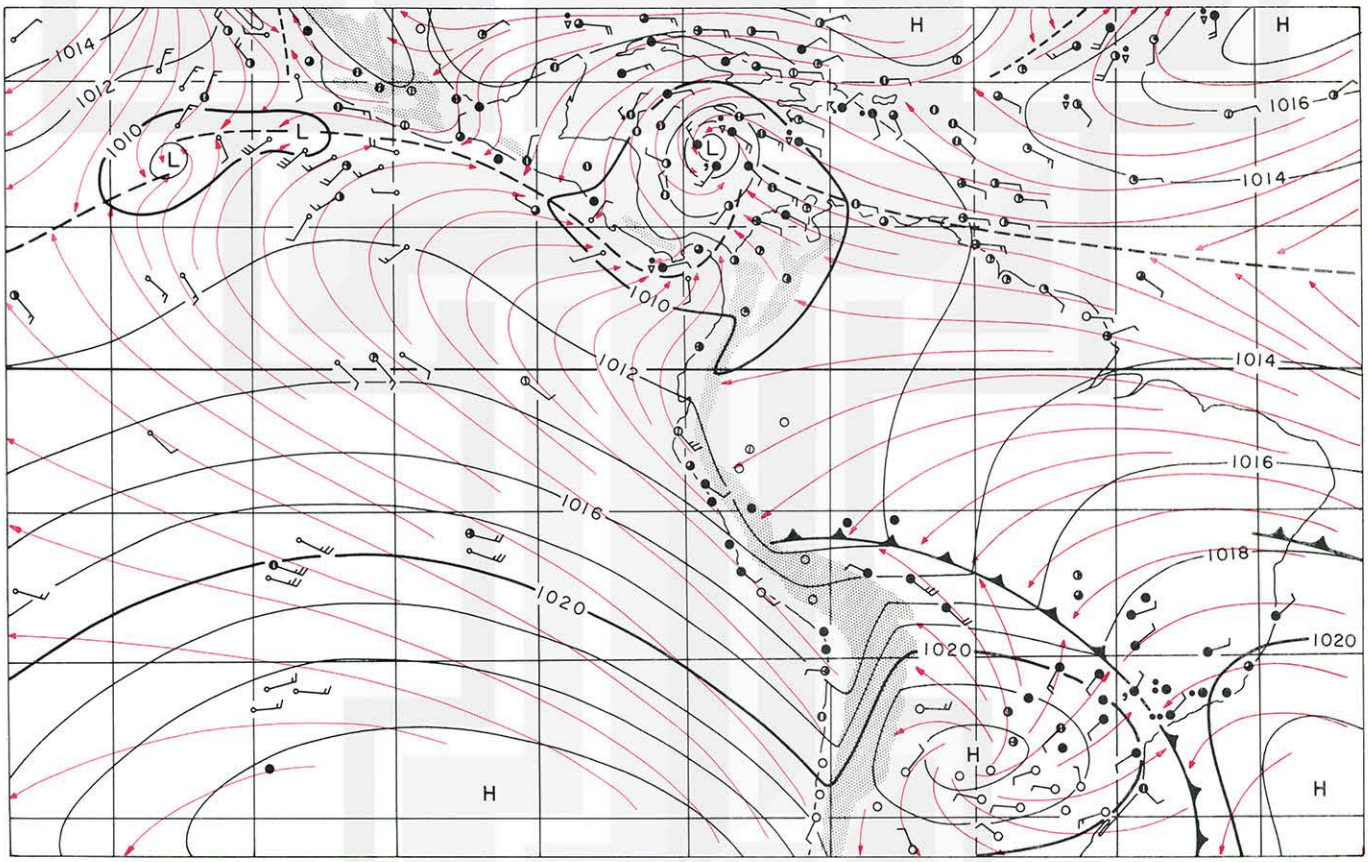

SEPTEMBER 14, 1967

The traveling anticyclone centered over the southern tip of Brazil cleared up vast areas in its west and south quadrants. A coastal cloud band near Sao Paulo is caused by the southerly flow as it undergoes orographic lifting along the coastal hills and mountains. The western end of the cold front is moving northward. Extensive cloud and rain areas are seen over the upper Amazon basin.

The ITCZ in the mid Atlantic is characterized by converging stream lines as well as a band of cloudiness. The intensification of northern hemisphere trade wind pushed the ITCZ over to northern Venezuela. North to northwesterly flow in the southwestern sector of Beulah also pushed the ITCZ down to Costa Rica.

Two cloud clusters in the Pacific are showing definite circulation patterns. However, they are too weak to be called hurricanes.

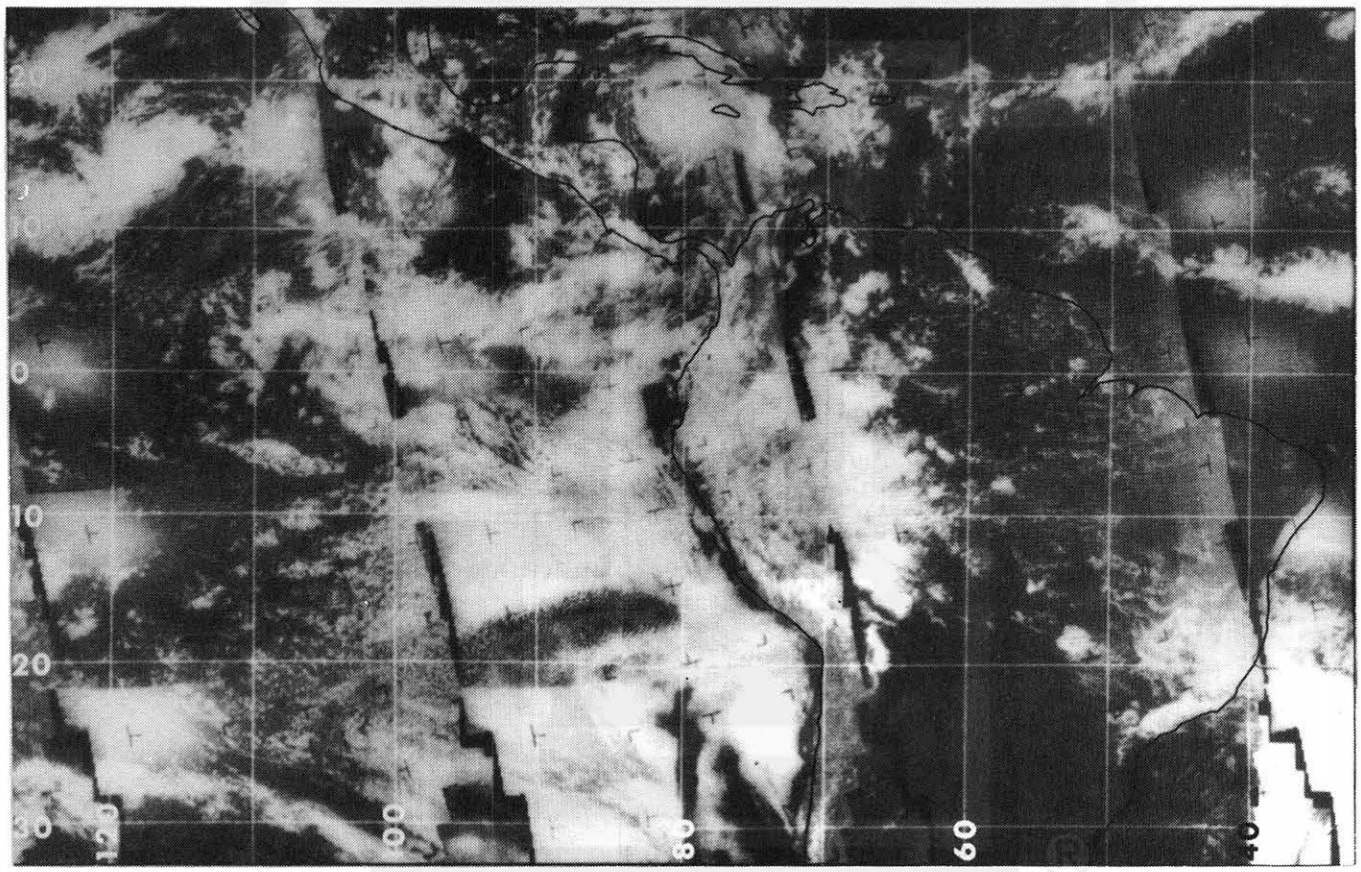

SEPTEMBER 14, 1967

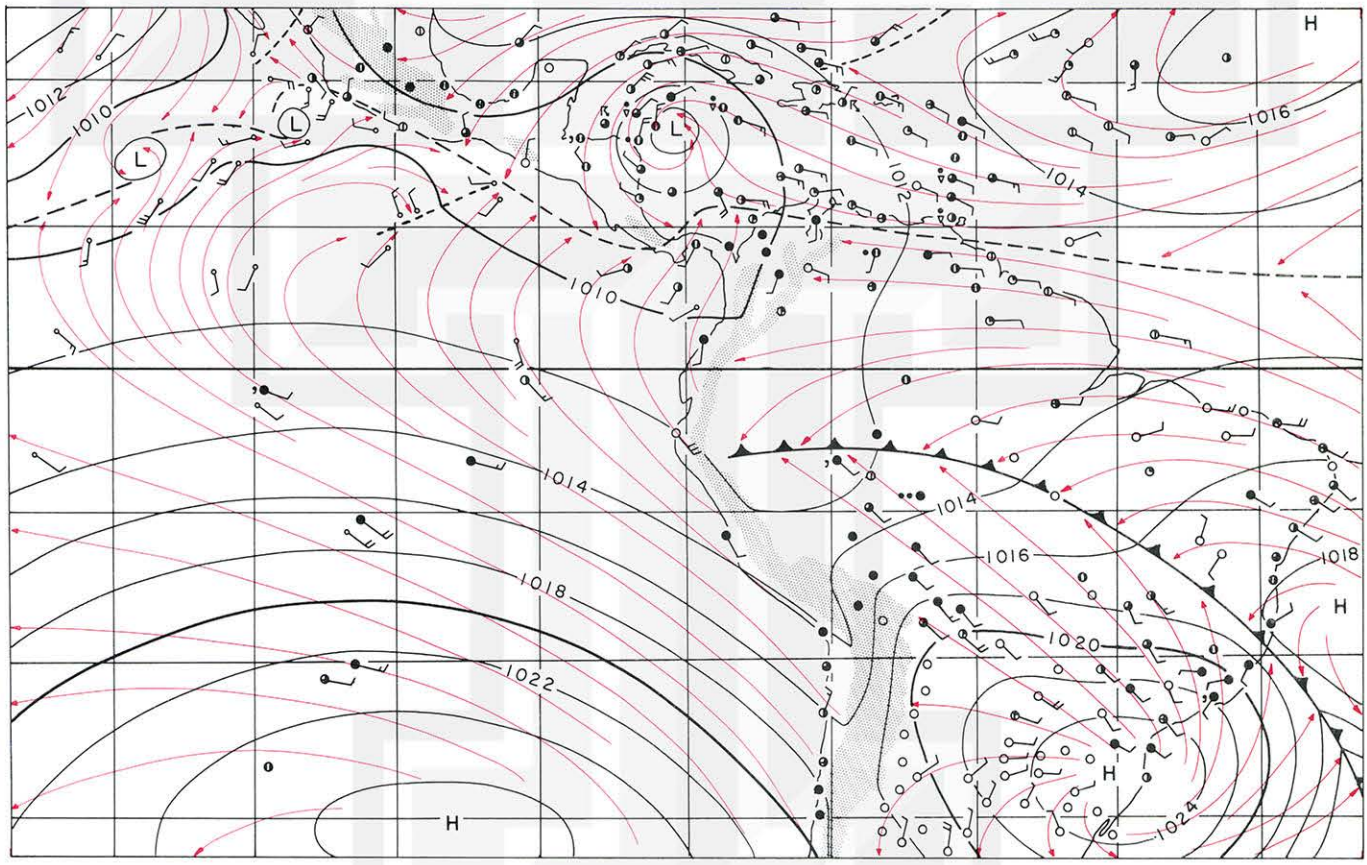

SEPTEMBER 15, 1967

As the cold front moved northeast, a large clear area extends from the upper Amazon basin to the entire Parana valley. Arc-shaped clouds over Asuncio and Sao Paulo are likely to be jet-stream cirrus. From the pattern of clearing and convective clouds, the western end of the cold front may be located just to the south of the equator.

A cloud cluster is seen to the northeast of Barbados. This cloud cluster is not associated with the ITCZ which runs along the northern coast of Venezuela. A significant convergence of cross-equatorial flow into a low over Panama is evident.

Beulah, while approaching Yucatan peninsula, grew into a strong hurricane with an extensive cirrus shield, 1000 km across. Two cloud clusters in the Pacific also developed into tropical depressions. An equatorial anticyclone appeared at 10 N and 110 W.

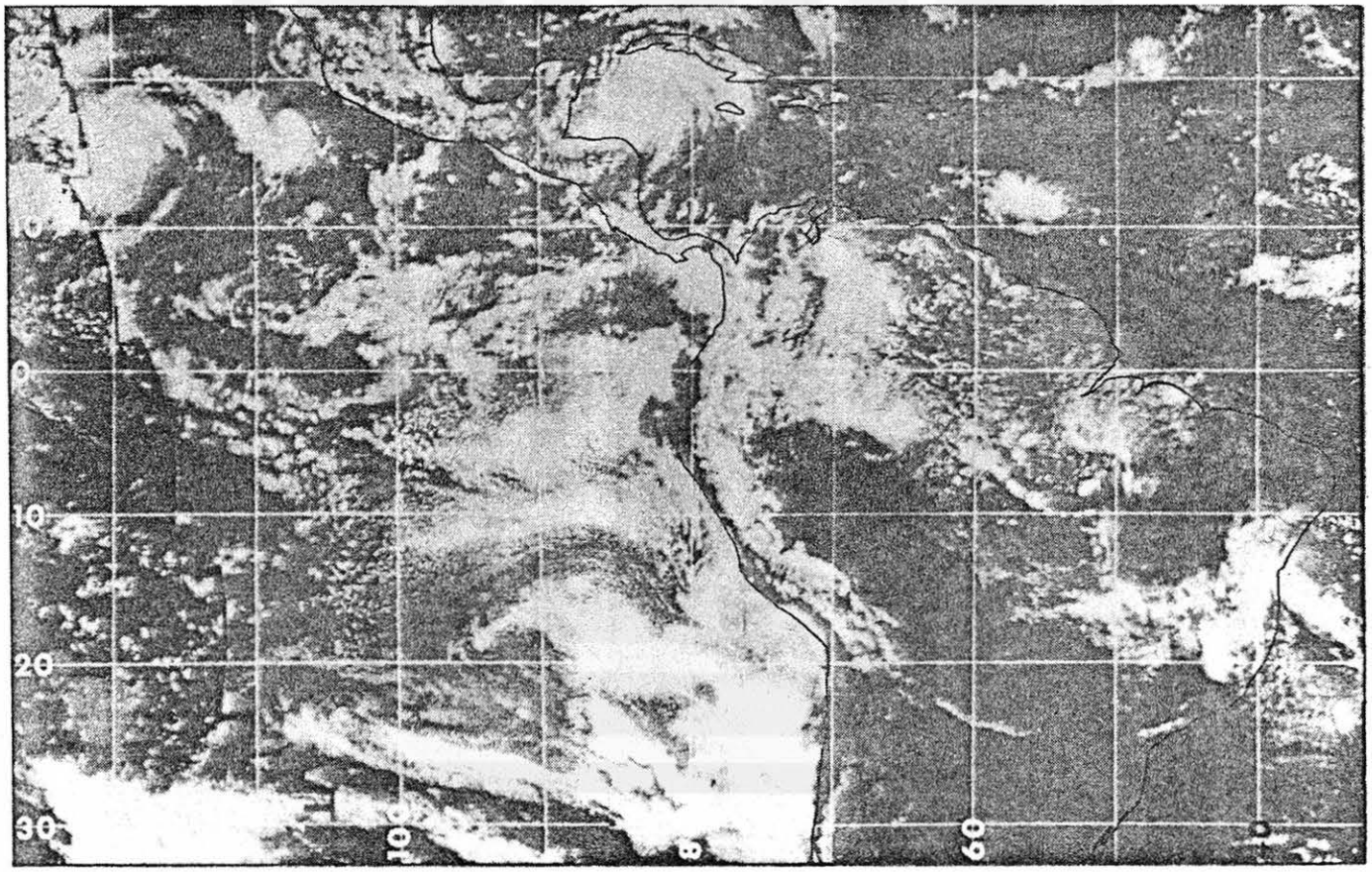

SEPTEMBER 15, 1967

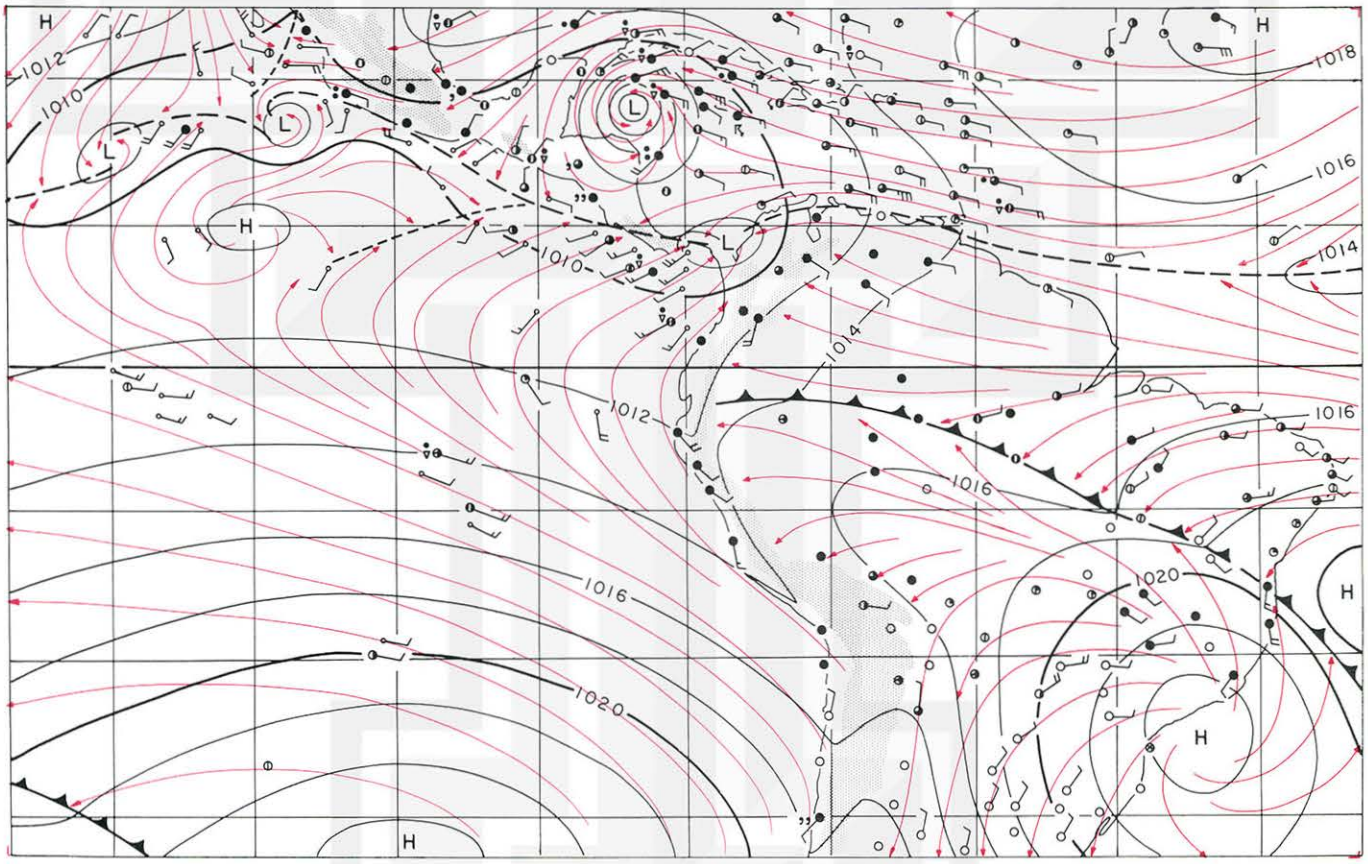

SEPTEMBER 16, 1967

Added to this chart are the cloud velocities computed from ATS 1 pictures. They are shown with short arrows pointing toward the direction of cloud motion. The equatorial anticyclone moved westward to 10N and 113W. While the western cloud cluster became a tropical cyclone.

Beulah intensified also. Cross-equatorial air is now blowing against the southeast coast of Central America, creating a band of cloudiness along the coast.

Over the South American continent, the cold front disintegrated suddenly, leaving a small portion over Bahia, Brazil. A cloud band perpendicular to the coast is a cold frontal cloud band. A low pressure center to the east of the Andes is developing, as a cold front approaches the low from the south.

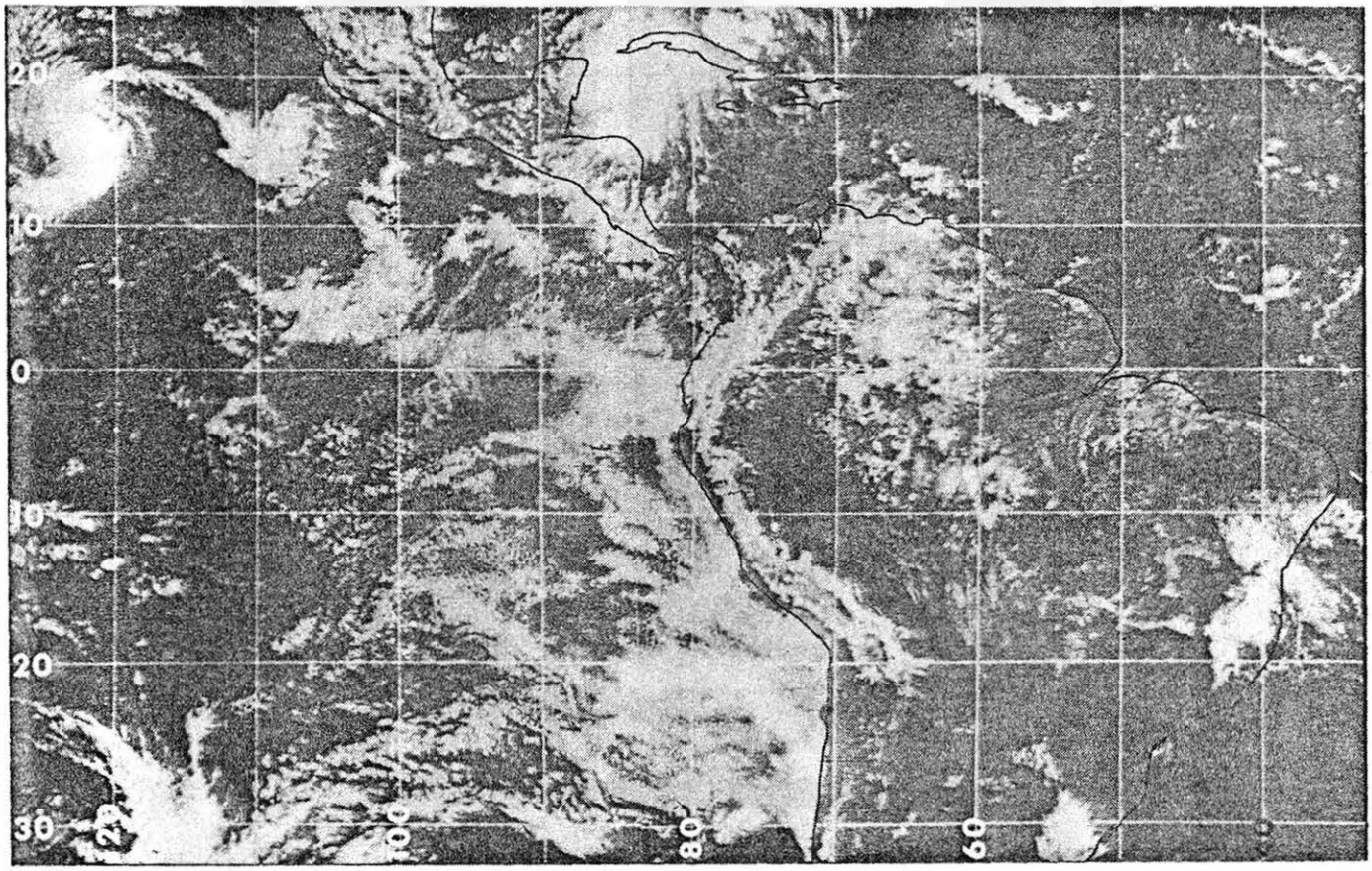

SEPTEMBER 16, 1967

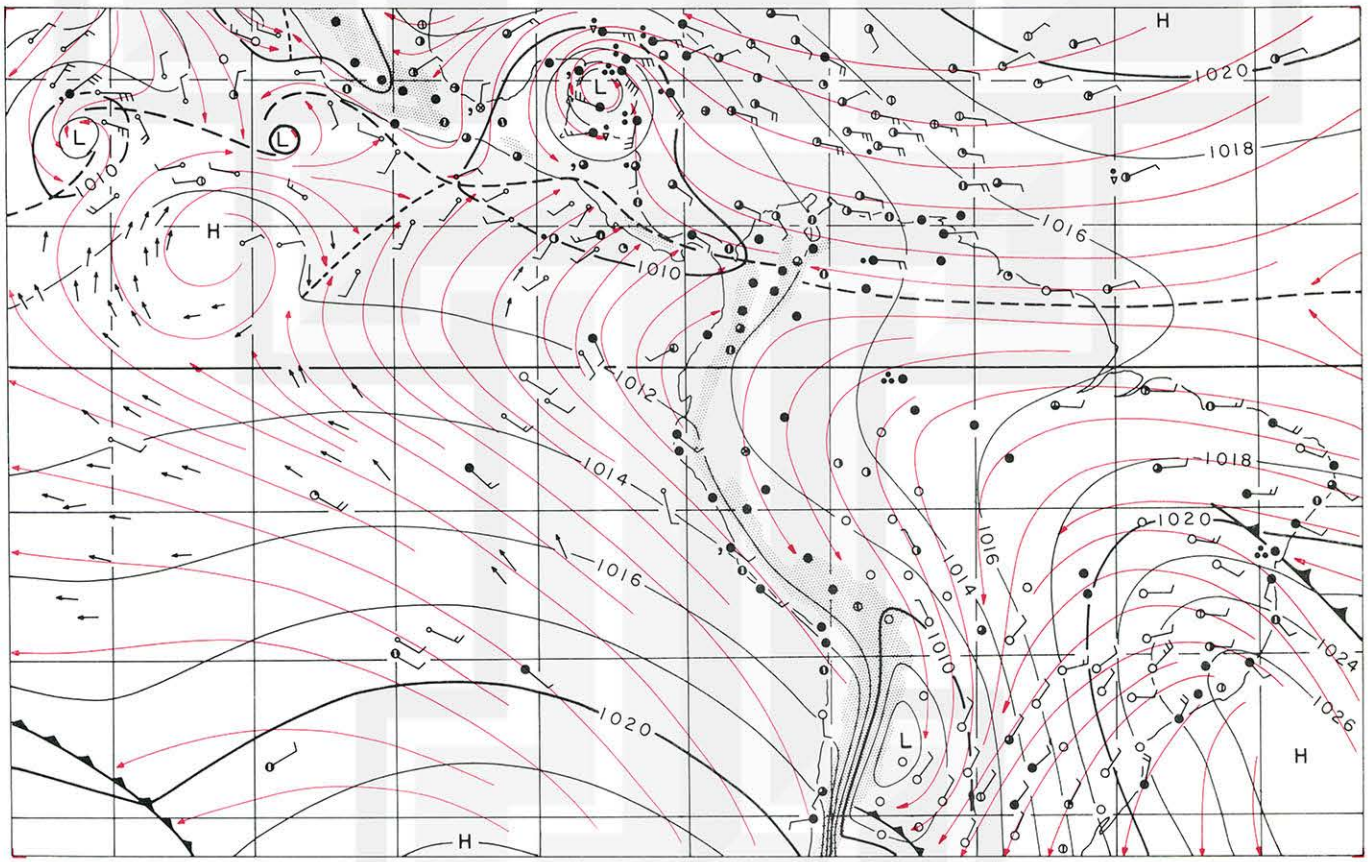

SEPTEMBER 17, 1967

The low pressure center is located over the Paraguay-Argentina border. It seems that all stream lines over Brazil are going into this low.

The ITCZ over the Atlantic became insignificant. However, the trade-wind boundary can be extended from the equatorial Atlantic to southern Guiana to central Colombia.

A depression over Panama has weakened with clearing around the center. Beulah became an intense hurricane, now located near Merida, Yucatan. Two tropical cyclones are seen in the Pacific. Each of the storms became so independent that their association with ITCZ can no longer be established.

Outflow from the equatorial anticyclone and the fresh flow from the southern hemisphere now meet along a short dashed line extending west-southwest from El Salvador. A narrow band of cloudiness is seen along the dashed line.

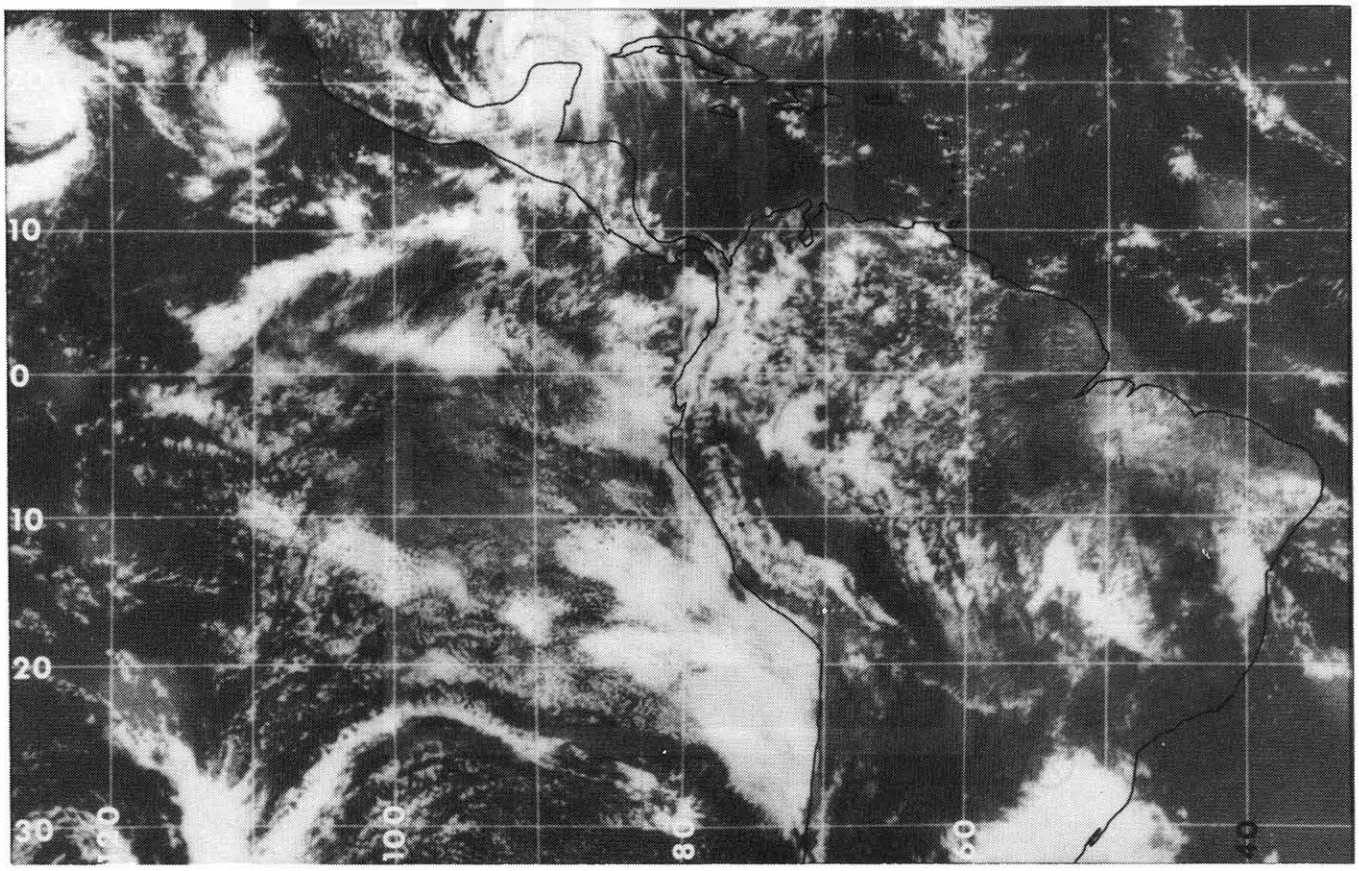

SEPTEMBER 17, 1967

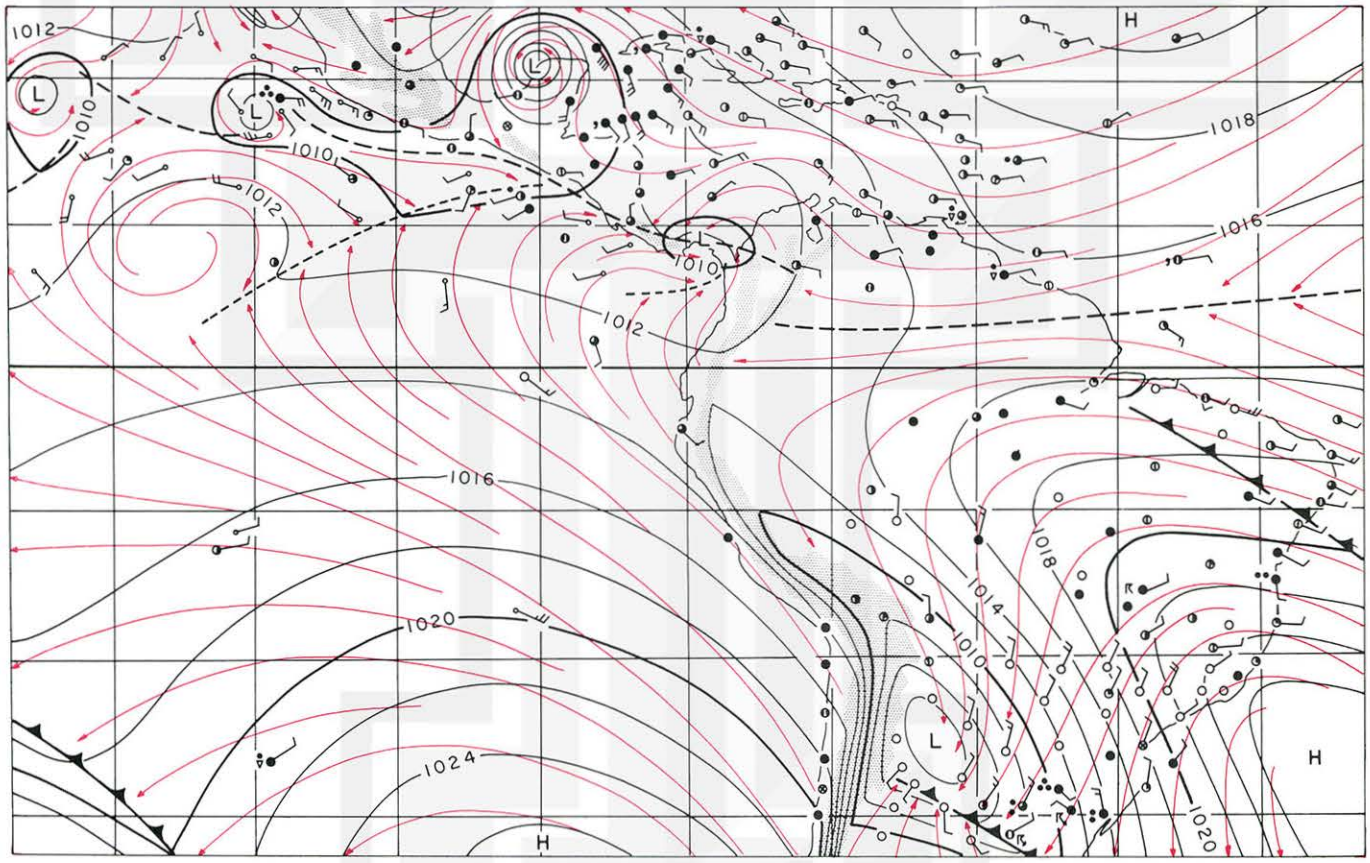

SEPTEMBER 18, 1967

A huge mesohigh superimposed upon a cold front is seen over Uruguay and vicinity. The mesohigh is characterized by a group of diverging stream lines. Most stations and ships inside the mesohigh reported heavy rain or thunderstorm. A cold front is seen over the Parana valley. It is of interest to see that the cold air behind the cold front is almost perpendicular to the isobars.

Small convective clouds are seen everywhere over Brazil, while large cells are seen in the equatorial region to the east of the Andes.

Beulah is in the Gulf of Mexico, approaching the coast of Texas. Two tropical storms in the Pacific became entirely independent systems, divorced practically from their parent ITCZ.

It should be noted that there are two convergence lines within the cross-equatorial flow. Both extend toward the west-southwest from El Salvador and Panama, respectively. Bright cloud bands are seen along these convergence lines.

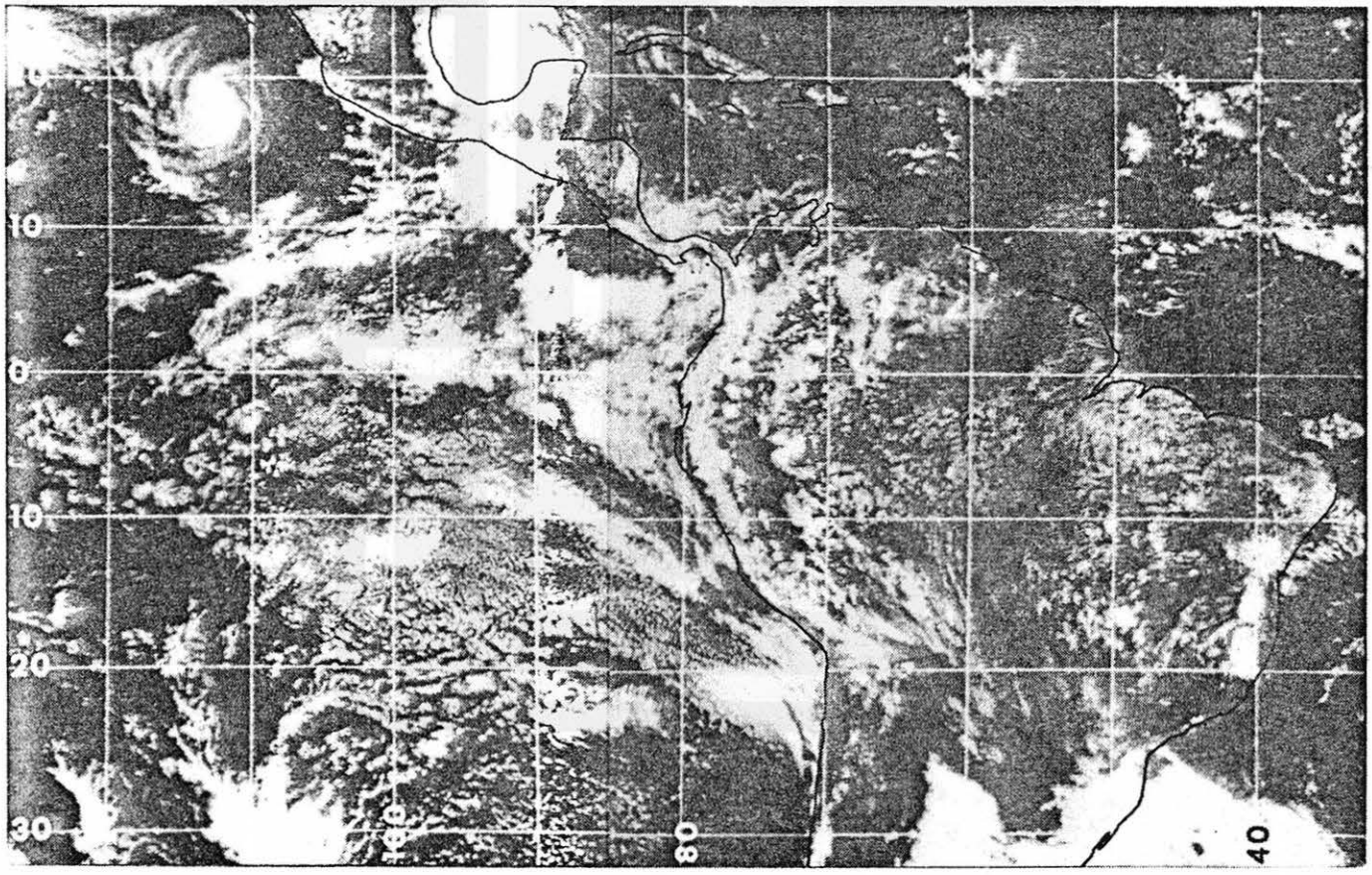

SEPTEMBER 18, 1967

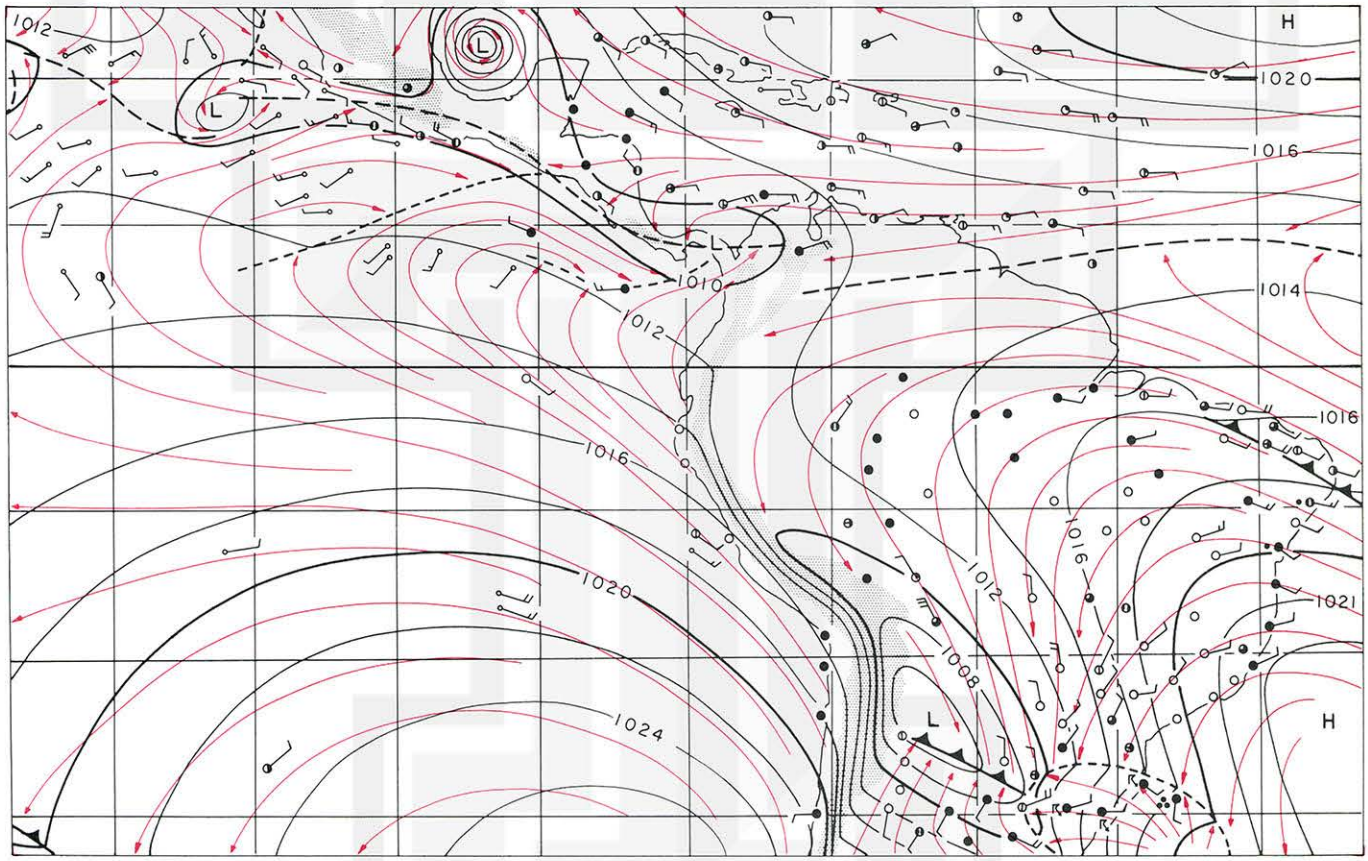

6. FLOW OF MOIST AIR

For the purpose of explaining the climatological patterns of clouds and precipitation, the flow of moist air during the 11-day analysis period was studied.

A wind-rose chart, thus prepared, is different from conventional ones which include frequency of wind regardless of its origin. This chart was made simply by excluding the frequency of polar air flow so as to give the frequency of the moist air flow.

It is seen that the moisture in the Amazon and Panama basins enters the continent across the northern coast of Brazil. Stream lines bend toward the south, creating a rain shadow E. Two rain shadows C and D are seen behind Cordiller. Oriental as the mountains block the easterlies.

Rain shadows A and B are quite apparent in the mean cloud-cover photograph for September.

F designates Atacama desert where annual rain is practically zero.

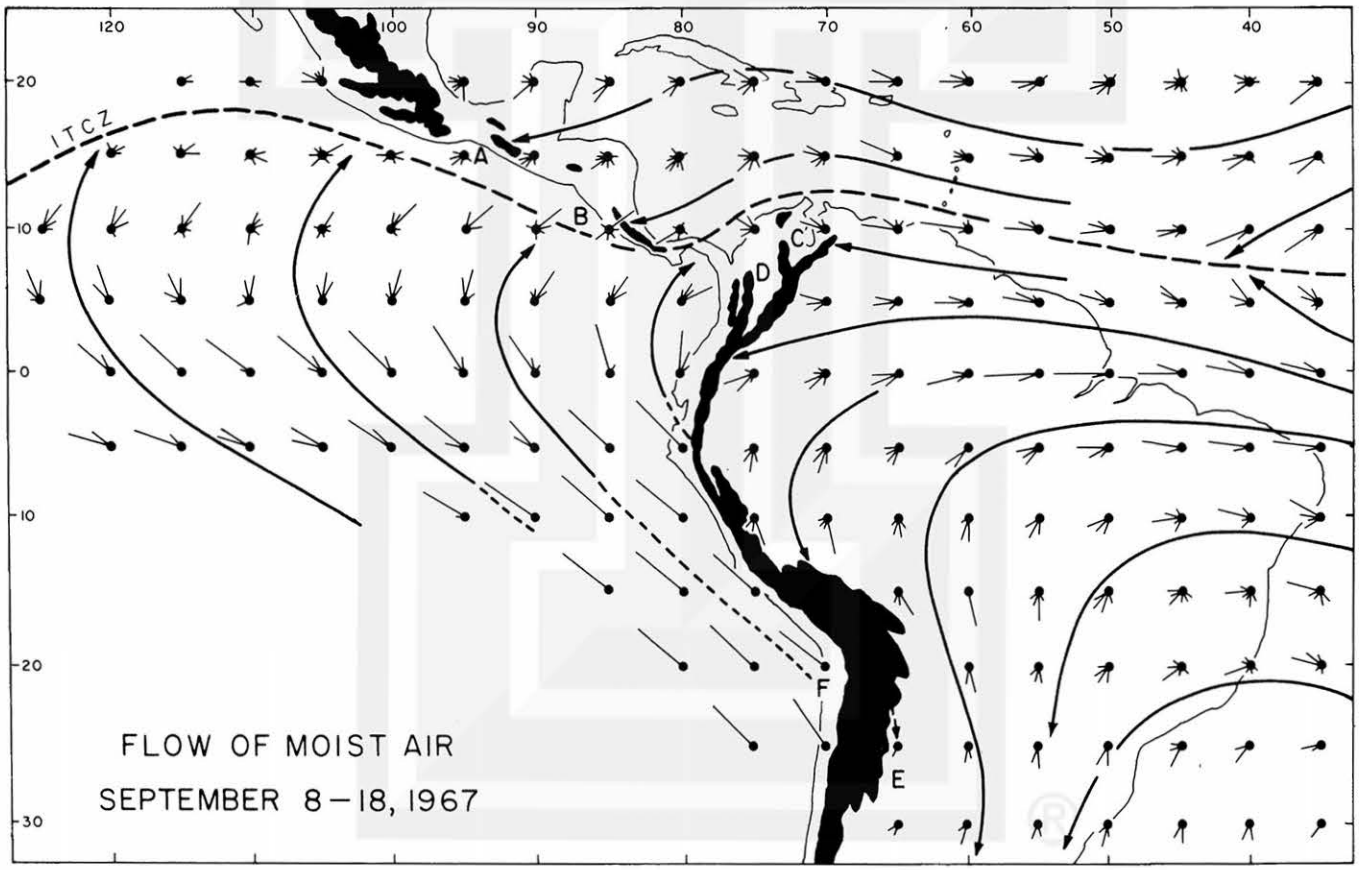

7. INTERPRETATION OF SEPTEMBER RAINFALL

In Guatemala and in Costa Rica, where two maxima are seen in the map, monthly rainfall of 797 and 691 mm, respectively, were reported. The satellite picture in Chapter 2 shows relatively clear areas to the east of these heavy rain areas where rain shadow can be expected.

Over 300 mm rainfall to the south of Panama was estimated from the mean cloud-cover picture. The area of this maximum extends west-northwest toward the Pacific south of Acapulco.

The axis of the isohyet pattern over the Atlantic runs from ITCZ in the mid Atlantic to Cuba. This is the region where hurricanes and easterly waves travel during the hurricane season.

Heavy rain, up to 330 mm, is seen over the upper Amazon and Orinoco basins. In the mountainous region of Cordillera Occidental and Oriental, rainfall drops to about 50 mm, showing a small minimum there.

Only 4 mm rainfall is recorded in northeast Brazil and practically none over the Atacama desert in northern Chile.

Thunderstorm days are over-printed in red. The highest thunderstorm frequency of 22 days is seen in the Amazon basin. In most other areas, several thunderstorm days are seen. One exception being the east coast of Brazil where orographic rain dominates.

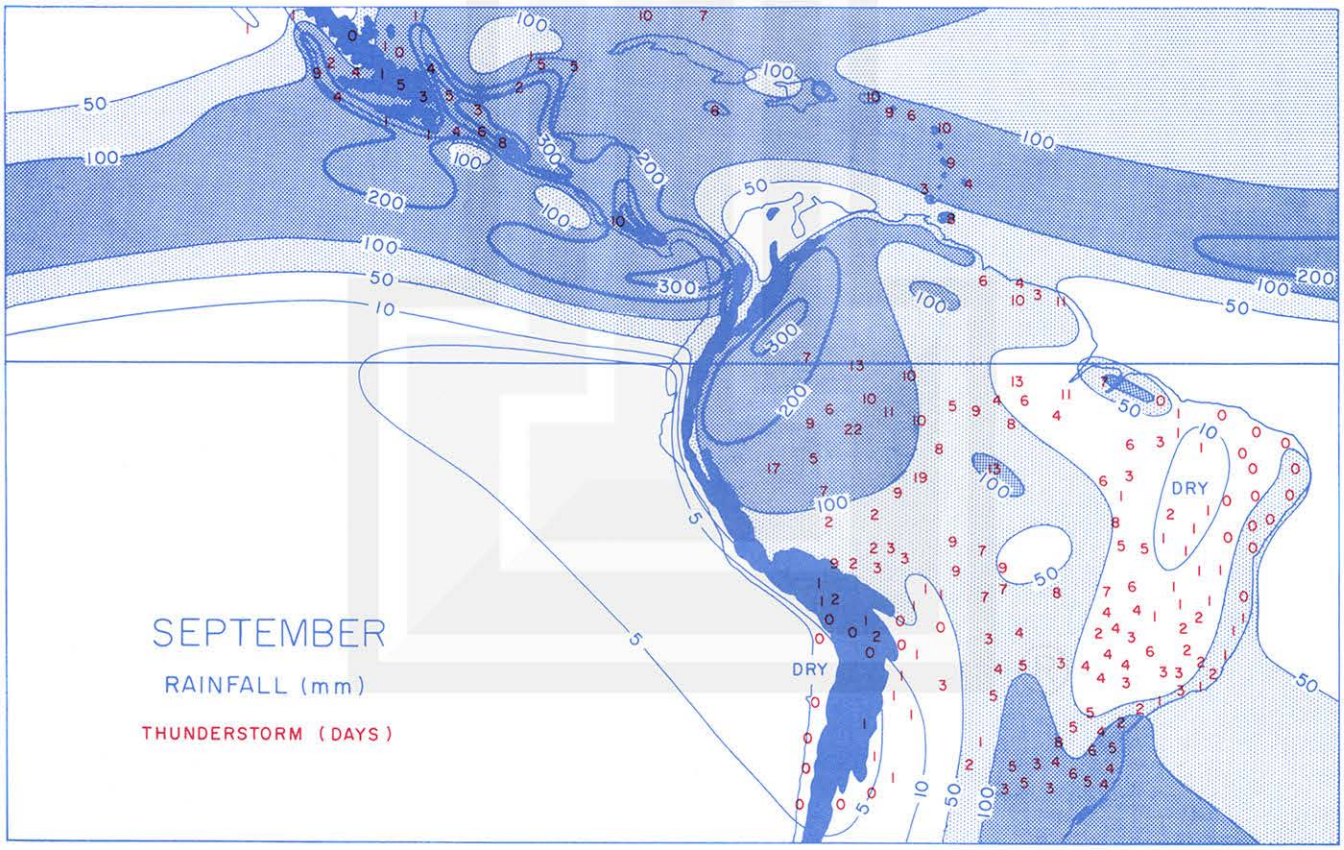

8. PRESSURE VARIATION ALONG THE WEST COAST

In order to determine the pressure variation within tropical Latin America, daily pressure was obtained from selected west coast stations as well as Islas Galapagos. In the tropics, pressure varies up and down practically in phase on both sides of the equator. Such a variation, 4 to 5 days in period, does not affect the local pressure gradient.

An abrupt change is seen between Antofagasta (23 40'S) and Quintero (32 48'S). The latter is under the influence of middle latitude pressure systems. A peak at Quintero on September 12 should be noted.

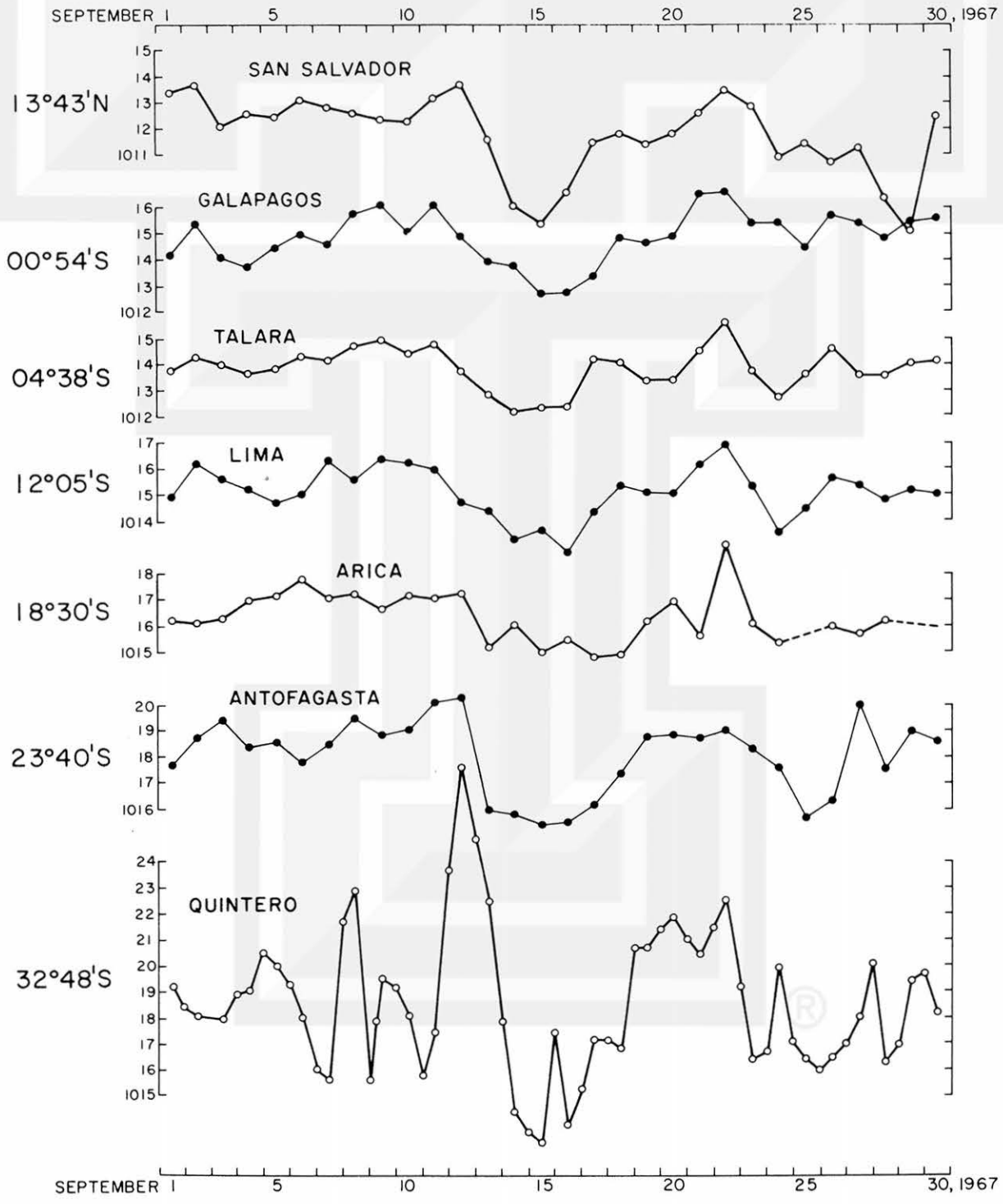

9. CONCLUSIONS

Tropical Latin America with an extremely complicated topography has long been unknown to meteorologists. The Andes Mountains, for instance, is the world's longest wall of high peaks, obstructing the east-west flow of low- and middle-level atmosphere.

The density of synoptic stations is not high enough to determine meteorological conditions in sub-synoptic scale. Moreover, the accuracy of the sea-level pressure from inland stations is not adequate for isobaric analysis because there will be very small pressure gradient within the tropics.

To overcome such difficulties in performing synoptic analyses, pictures from various satellites are of extreme value. Resolution of the present and future meteorological satellite is in the order of one mile, making it possible to detect even a small convective cloud floating over the Amazon jungles, Andes Mountains, middle of the Ocean, etc.

Analytical results presented herein will be useful for their application to other months of the year, if satellite and synoptic data can be combined in a similar manner.

MESOMETEOROLOGY PROJECT - - - RESEARCH PAPERS

(Continued from front cover)

42.* A Study of Factors Contributing to Dissipation of Energy in a Developing Cumulonimbus - Rodger A. Brown and Tetsuya Fujita

43. A Program for Computer Gridding of Satellite Photographs for Mesoscale Research - William D. Bonner

44. Comparison of Grassland Surface Temperatures Measured by TIROS VII and Airborne Radiometers under Clear Sky and Cirriform Cloud Conditions - Ronald M. Reap

45. Death Valley Temperature Analysis Utilizing Nimbus I Infrared Data and Ground-Based Measurements - Ronald M. Reap and Tetsuya Fujita

46. On the "Thunderstorm-High Controversy" - Rodger A. Brown

47. Application of Precise Fujita Method on Nimbus I Photo Gridding - Lt. Cmd. Ruben Nasta

48. A Proposed Method of Estimating Cloud-top Temperature, Cloud Cover, and Emissivity and Whiteness of Clouds from Short- and Long-wave Radiation Data Obtained by TIROS Scanning Radiometers - T. Fujita and H. Grandoso

49. Aerial Survey of the Palm Sunday Tornadoes of April 11, 1965 - Tetsuya Fujita

50. Early Stage of Tornado Development as Revealed by Satellite Photographs - Tetsuya Fujita

51. Features and Motions of Radar Echoes on Palm Sunday, 1965 - D. L. Bradbury and T. Fujita

52. Stability and Differential Advection Associated with Tornado Development - Tetsuya Fujita and Dorothy L. Bradbury

53. Estimated Wind Speeds of the Palm Sunday Tornadoes - Tetsuya Fujita

54. On the Determination of Exchange Coefficients: Part II - Rotating and Nonrotating Convective Currents - Rodger A. Brown

55. Satellite Meteorological Study of Evaporation and Cloud Formation over the Western Pacific under the Influence of the Winter Monsoon - K. Tsuchiya and T. Fujita

56. A Proposed Mechanism of Snowstorm Mesojet over Japan under the Influence of the Winter Monsoon - T. Fujita and K. Tsuchiya

57. Some Effects of Lake Michigan upon Squall Lines and Summertime Convection - Walter A. Lyons

58. Angular Dependence of Reflection from Stratiform Clouds as Measured by TIROS IV Scanning Radiometers - A. Rabbe

59. Use of Wet-beam Doppler Winds in the Determination of the Vertical Velocity of Raindrops inside Hurricane Rainbands - T. Fujita, P. Black and A. Loesch

60. A Model of Typhoons Accompanied by Inner and Outer Rainbands - Tetsuya Fujita, Tatsuo Izawa,, Kazuo Watanabe and Ichiro Imai

61. Three-Dimensional Growth Characteristics of an Orographic Thunderstorm System - Rodger A. Brown

62. Split of a Thunderstorm into Anticyclonic and Cyclonic Storms and their Motion as Determined from Numerical Model Experiments - Tetsuya Fujita and Hector Grandoso

63. Preliminary Investigation of Peripheral Subsidence Associated with Hurricane Outflow - Ronald M. Reap

64. The Time Change of Cloud Features in Hurricane Anna, 1961, from the Easterly Wave Stage to Hurricane Dissipation - James E. Arnold

65. Easterly Wave Activity over Africa and in the Atlantic with a Note on the Intertropical Convergence Zone during Early July 1961 - James E. Arnold

66. Mesoscale Motions in Oceanic Stratus as Revealed by Satellite Data - Walter A. Lyons and Tetsuya Fujita

67. Mesoscale Aspects of Orographic Influences on Flow and Precipitation Patterns - Tetsuya Fujita

68. A Mesometeorological Study of a Subtropical Mesocyclone -Hidetoshi Arakawa, Kazuo Watanabe, Kiyoshi Tsuchiya and Tetsuya Fujita

69. Estimation of Tornado Wind Speed from Characteristic Ground Marks - Tetsuya Fujita, Dorothy L. Bradbury and Peter G. Black

70. Computation of Height and Velocity of Clouds from Dual, Whole-Sky, Time-Lapse Picture Sequences - Dorothy L. Bradbury and Tetsuya Fujita

71. A Study of Mesoscale Cloud Motions Computed from ATS-I and Terrestrial Photographs - Tetsuya Fujita, Dorothy L. Bradbury, Clifford Murino and Louis Hull

72. Aerial Measurement of Radiation Temperatures over Mt. Fuji and Tokyo Areas and Their Application to the Determination of Ground- and Water-Surface Temperatures - Tetsuya Fujita, Gisela Baralt and Kiyoshi Tsuchiya

73. Angular Dependence of Reflected Solar Radiation from Sahara Measured by TIROS VII in a Torquing Maneuver - Rene Mendez.

74. The Control of Summertime Cumuli and Thunderstorms by Lake Michigan During Non-Lake Breeze Conditions - Walter A. Lyons and John W. Wilson

75. Heavy Snow in the Chicago Area as Revealed by Satellite Pictures - James Bunting and Donna Lamb

76. A Model of Typhoons with Outflow and Subsidence Layers - Tatsuo Izawa

* out of print

(continued on outside back cover)